DEPARTMENT OF THE INTERIOR
U.S. GEOLOGICAL SURVEY

Genesis and evolution of the Baid Al Jimalah tungsten deposit, Kingdom of Saudi Arabia

by

Robert J. Kamilli[1/]

Open-File Report 86-588

Report prepared by the U.S. Geological Survey in cooperation with the Deputy Ministry for Mineral Resources, Saudi Arabia

This report is preliminary and has not been reviewed for conformity with U.S. Geological Survey editorial standards and stratigraphic nomenclature.

1/ USGS, Saudi Arabian Mission

1986

CONTENTS

ILLUSTRATIONS

TABLES

GENESIS AND EVOLUTION OF THE BAID AL JIMALAH TUNGSTEN DEPOSIT, KINGDOM OF SAUDI ARABIA

by

Robert J. Kamilli[1/]

ABSTRACT

The Baid al Jimalah tungsten deposit (lat 25°09' N., long 42°41' E.) is a swarm of steeply dipping, sheeted, tungsten-bearing quartz veins. It is spatially, temporally, and genetically associated with a 569 Ma, highly differentiated, porphyritic granite that intrudes late Proterozoic, immature sandstones of the Murdama group.

The bulk of the vein constituents came from hydrothermal fluids exsolved from a granite cupola at a depth of about 3.1 km during a single cycle of magma intrusion and hydrothermal mineralization. Hypogene mineralization can be divided into 3 main periods: early quartz-molybdenite stockwork veins, wolframite- and scheelite-bearing greisen veins, and late, barren veins. Each of the three periods can be divided into several stages that are transitional to each other. The greisen veins, in particular, show replacement of earlier mineral assemblages by later ones. The veins at Baid al Jimalah East, approximately 1.5 km to the east of the Baid al Jimalah tungsten deposit, are genetically related to it and probably formed while the greisen mineralization was being deposited.

Early stockwork mineralization was formed near magmatic temperatures (580°-700° C) from low salinity fluids (1-2 weight percent NaCl equivalent). Two fluids were present, one low density and CO_2 rich, the other high density and H_2O rich. Greisen mineralization was formed from fluids in the liquid state at temperatures mostly between 390° and 430° C with salinities between 4.5 and 10.9 weight percent NaCl equivalent. Late, barren mineralization formed from liquids with salinities between 0.5 and 3.0 weight percent NaCl equivalent and at temperatures at least as low as 238° C. The veins at Baid al Jimalah East formed from liquids between 0 and 4.2 weight percent NaCl equivalent at temperatures largely between 300° and 375°C. Depth of mineralization was greater than 3.1 km. The temperatures given above have been corrected for pressure assuming this depth, and are 75-80°C higher than the fluid inclusion filling temperatures. Important volatile constituents of the hydrothermal fluids were CO_2 and CH_4, in addition to H_2O and HF.

Baid al Jimalah is similar in character and origin to other tungsten-tin greisen deposits in the world, especially the Hemerdon deposit in Devon, England. It is also analogous to Climax-type molybdenum deposits, which contain virtually identical mineral assemblages, but with the relative intensities of the molybdenum and tungsten mineralization reversed.

1/ USGS Saudi Arabian Mission

INTRODUCTION

The Baid al Jimalah tungsten deposit was discovered in 1980 by J. Cole, of the U.S. Geological Survey, during reconnaissance geologic mapping. In 1983, E. A. DuBray, also of the U.S. Geological Survey, discovered the Jabal as Silsilah tin deposit, 110 km to the north of Baid al Jimalah. Both deposits are associated with late Protereozoic, highly differentiated granites that have undergone intense greisen alteration, yet these two deposits are markedly dissimilar in a number of ways. The Baid al Jimalah deposit consists primarily of sheeted, quartz-rich, wolframite-bearing veins that cut both granite and country rock over an area of approximately 1 km^2. The Jabal as Silsilah deposit occurs as disseminated mineralization within the tops of numerous, small cupolas covering an area about 9 km^2. The presence of these two barely exposed, potentially economic deposits holds promise for the discovery of additional, similar deposits in the northeastern Arabian Shield The purpose of this report is to develop a genetic model for the Baid al Jimalah deposit that can be profitably used in the exploration for similar deposits in Saudi Arabia. There is a companion report on Jabal as Silsilah (Kamilli, in press). The objective of these studies is to establish the similarities and differences between Baid al Jimalah and Jabal as Silsilah. Such information will permit the refinement of any exploration model for tin/tungsten deposits by the identification of features that are the result of local geology and those that are general characteristics of any such undiscovered deposits in the region.

ACKNOWLEDGEMENTS

This report is based on work completed by agreement between the U.S. Geological Survey and the Saudi Arabian Ministry of Petroleum and Mineral Resources under subproject 3.12.05 of the annual work program of the Deputy Ministry for Mineral Resources. Special thanks go to the geological staff of Riofinex Limited, who made available all drill core and allowed access to all data collected during their economic evaluation of Baid al Jimalah.

Early drafts of this report were reviewed and improved by Willis H. White and Gary Landis. The author has benefitted greatly from discussions with J. C. Cole, E. A. Du Bray, T. J. Reynolds and W. H. White. J. S. Stuckless provided the chemical analyses of samples from the Baid al Jimalah granite.

GEOLOGIC SETTING AND PROSPECT GEOLOGY

INTRODUCTION

The Baid al Jimalah deposit is located in the Al Jurdhawiyah quadrangle (sheet 25/42 D) at lat 25°09' N., long 42°41" E. It is divided into two separate zones: Baid al Jimalah West (MODS 2661), a tungsten-bearing deposit: and Baid al Jimalah East (MODS 960), a much smaller gold-base-metal zone, located 1.5 km to the east (fig. 1).

Baid al Jimalah East was the original discovery of mineralization in the area (Fakhry, 1941; Mytton, 1970) and is situated in a group of low hills with an average elevation 900 - 950 m (fig. 2). The name was formerly transliterated as "Bede el Gemela". The deposit consists of a series of sub-parallel veins that

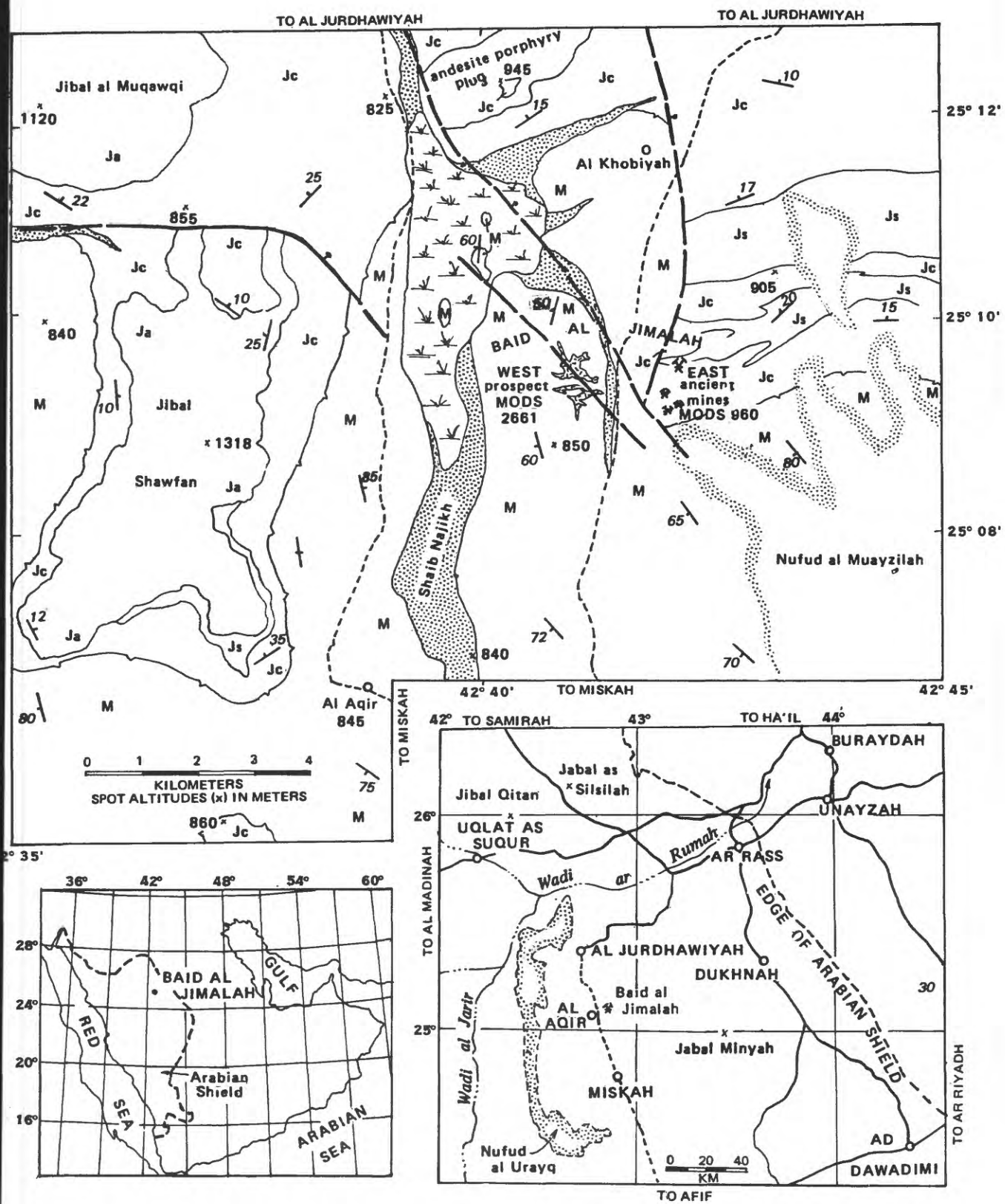

Figure 1.--*Maps showing location of the Baid al Jimalah deposit and subregional geology in the vicinity. Symbols in the upper diagram denote Murdama group (M), Jurdhawiyah group volcaniclastic conglomerate (Jc), volcaniclastic sandstone (Js), and andesite (Ja); basal unconformity of Jurdhawiyah group indicated by contact with carets. Bar-and-ball on downthrown side of faults. Principal auto tracks indicated by short-dash lines. (from Elliott and Cole, 1986).*

strike from N. 55 W. to N. 70 W., most of which are narrow and discontinuous, with little or no alteration envelopes in the wall-rock. The principal ancient working is at the northern edge of the area and can be as wide as 7 m, although the vein at its widest point is less than 2 m. The vein has a strike of N. 65 W. and a dip of 75° S. The area is characterized by ancient trenches and slag heaps. Radiocarbon determinations on charcoal, obtained by Riofinex, yielded an age of 1140±80 years B.P. There seems to be more slag present than can be accounted for by the visible trenches, suggesting that additional ore was mined elsewhere.

The veins and granite of Baid al Jimalah West, the principal subject of this report, are well-exposed along two WNW-trending ridges in the east side of the Shaib Najikh valley (figs. 1, 2, 3, and 4). The highest-grade portion of the deposit is more resistant to erosion and gives rise to hills of low relief over the WNW-striking veins and associated greisen alteration. The average elevation of the valley floor is 845 m and the highest elevation on the ridges is 860 m. Information on the geology and mineralization of the area was obtained from 11 trenches dug by the USGS, and 6 diamond drill holes and 18 air-flush percussion holes drilled by Riofinex (fig. 4).

REGIONAL SETTING

Most of the the geologic setting has been summarized from Elliott and Cole (1986) and is included in this report to provide a geologic context for the studies reported here. Further details may be found in Cole and others (1981) and Lofts (1982).

The Baid al Jimalah deposit is located in the northeastern part of the late Proterozoic Arabian Shield. The associated granite was emplaced at 569±16 Ma into regionally folded, fine-grained feldspathic sandstone of the Murdama group (approximately 670 - 655 Ma) Cole and Hedge, 1986). The veins of Baid al Jimalah East cut rocks of the Jurdhawiyah group (approximately 640 - 625 Ma; Cole and Hedge, 1986), that unconformably overlies rocks of the Murdama group and is composed of slightly folded, homoclinal conglomerate, sandstone, and andesite.

The porphyritic granite of Baid al Jimalah is similar to other, late Proterozoic, peraluminous granites in the region, all of which have been assigned to the Abanat suite (Cole, 1985a, b). The rocks of the Abanat suite are part of a much larger group of "anorogenic" granites that intruded the Arabian Shield near the end of the the Pan-African orogeny (Stoeser and Camp, 1984).

PROSPECT GEOLOGY

Structure

The Baid al Jimalah West deposit sits astride a N. 45° W. shear zone that is located primarily in a swale between the north and south ridges. (fig. 4). The shear zone extends at least 2.5 km to the NW and 1.5 km to the SE, and Riofinex geologists claim to have traced it for about 10 km in both directions (Lofts, 1982). A minor, subparallel strand can be seen to the north. Projection of the main shear zone downward to its intersection with diamond drill hole BAJ-2 gives a dip of 65° SW. The shear zone clearly was an important control on the deposit, and was

Figure 2.--*Oblique aerial photograph of principal trench at Baid al Jimalah East, looking west-southwest toward Baid al Jimalah West and Jabal Shawfan.*

Figure 3.--*Oblique aerial photograph of Baid al Jimalah West, looking southeast, showing trenches.*

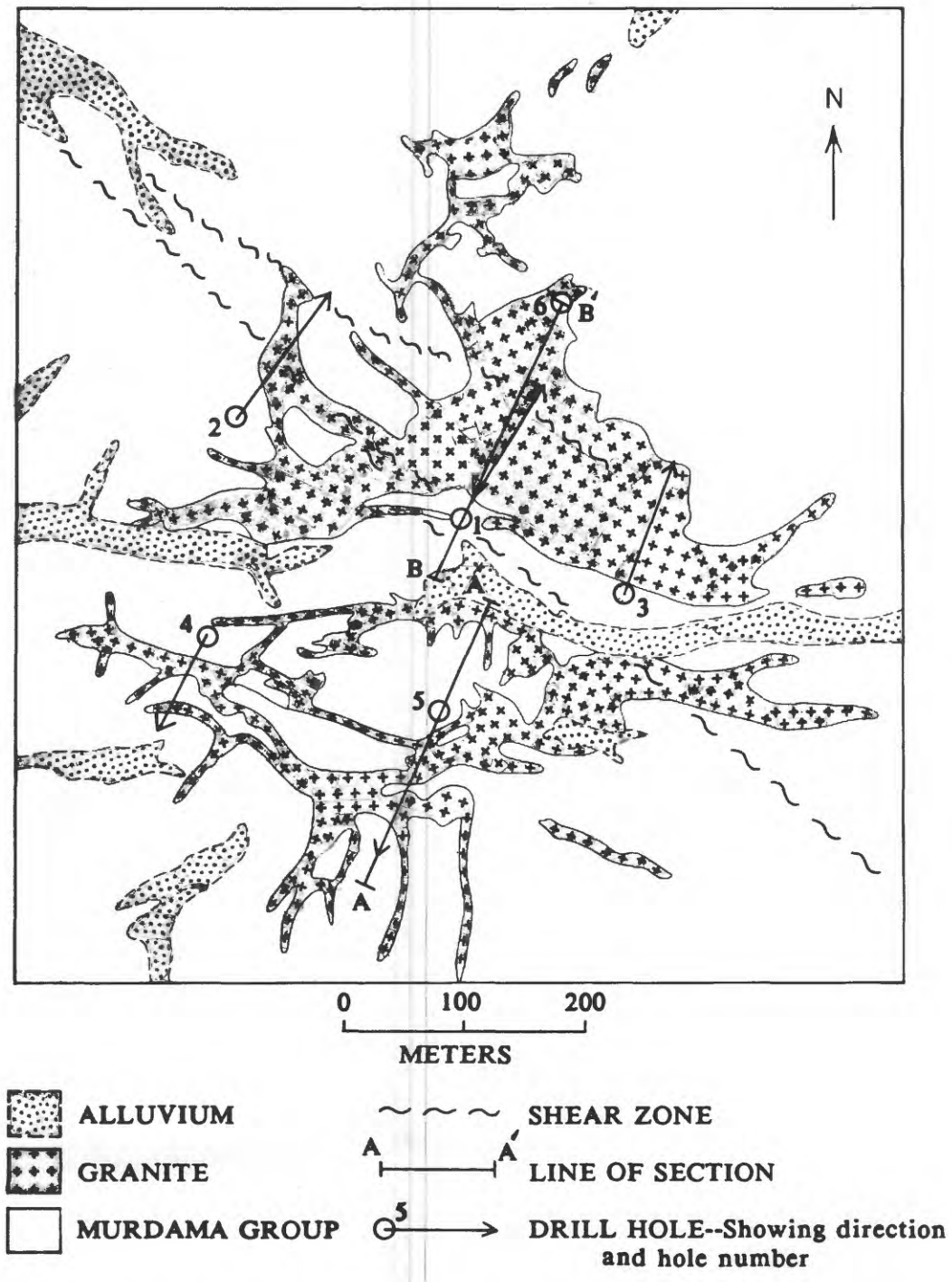

Figure 4.--*Geologic sketch map of the Baid al Jimalah West tungsten deposit, showing locations of trenches, drill holes, and line of section for plate 1 (modified from Elliott and Cole, 1986).*

active before, during, and after the emplacement and associated mineralization of the Baid al Jimalah granite. The fact that the shear zone existed at the time of intrusion is proven by the presence of an aplite dike in the structure about 0.5 km NW of the Baid al Jimalah granite. The shear zone also contains quartz veins, and is the locus of late mineralization.

The shear zone roughly coincides with a broad, anticlinal warp in the unconformable base of the Jurdawiyah group (Lofts, 1982), and may mark an active structural hinge line during Jurdhawiyah time. Lofts considers this fault to be part of the regional Najd system of Moore (1979), however Kleinkopf and Cole (1982) point out that major transcurrent slip on Najd faults in the region ended about 620 Ma, which is 50 Ma before the intrusion of the Baid al Jimalah granite.

The dominant N. 60^{o}-75^{o} W. alignment of the veins at Baid al Jimalah East and the major veins at Baid al Jimalah West implies a strong control by the shear zone during mineralization. The 15^{o} angle between the dominant vein trend and the strike of the shear zone, as well as the apparent horsetailing of some of the veins at Baid al Jimalah West against the shear zone, strongly implies that shear stresses formed the dominant vein trend. These structures are essentially dilational tension joints formed in the manner described by Riedel (1929). Other veins that are not parallel to the main trend probably formed as a result of early hydrofracturing (discussed later) or the intrusion and cooling of the granite. Despite its importance on the evolution of the ore deposit, this shear zone does not show any evidence of displacement, neither of the granite nor of geophysical and geochemical anomalies (Lofts, 1982).

Rock descriptions

Rocks in the immediate vicinity of Baid al Jimalah (oldest to youngest) are: Murdama sandstone, diabase dikes and sill-like bodies, volcanic and volcaniclastic rocks of the Jurdhawiyah group, granodiorite porphyry of the Idah suite (620±5 Ma; Cole and Hedge, 1986), and the Baid al Jimalah granite.

The Murdama rocks have been metamorphosed to greenschist facies and consist chiefly of fine-grained, immature sandstone that has abundant clasts of metamorphosed intermediate and felsic volcanic rock, plagioclase, and quartz in a matrix of chlorite, granular epidote, blastic calcite, pyrite, and pyrrhotite (Cole, 1981, 1985b). Within a 750 m contact aureole of the granite, Murdama sandstone is metamorphosed to hornfels, composed of quartz, plagioclase, alkali feldspar, brown biotite, cordierite, muscovite, and opaque minerals. Much of the muscovite and all the fluorite reported by Elliott and Cole (1986) probably formed during greisenization and not during contact metamorphism.

Black, fine-grained "diabase" dikes and sill-like bodies are visible on the surface at Baid al Jimalah West and have been logged in diamond drill holes BAJ-1, 2, 3, and 5. This rock contains approximately 50 percent plagioclase, both in the groundmass and as 5 mm laths; 30 percent biotite; approximately 10 percent quartz; and minor amounts of alkali feldspar, opaque minerals, plus hydrothermal muscovite, sulfides, and fluorite. No original pyroxene or amphibole exists. Lofts (1982) speculates that the rock was originally andesitic.

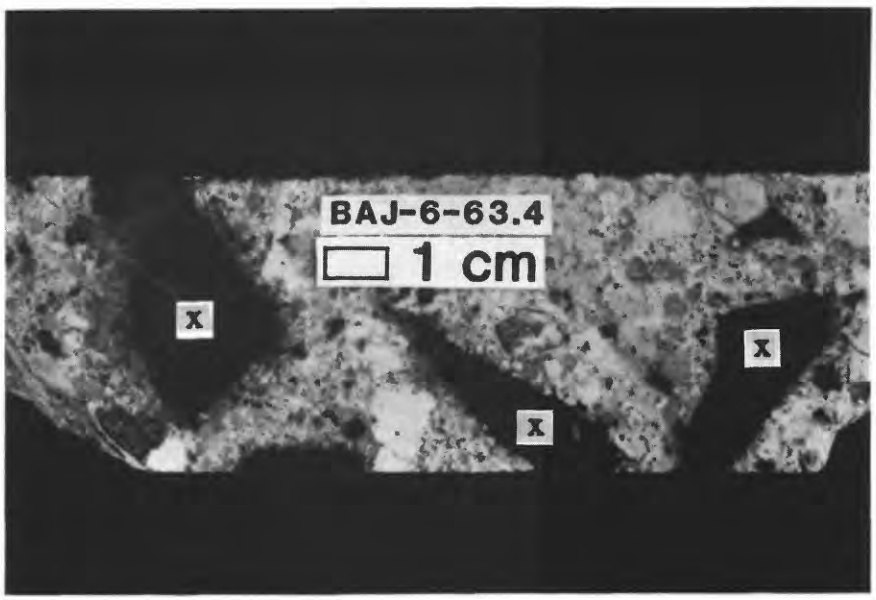

Figure 6.--*Photograph of typical Baid al Jimalah granite with xenoliths (x) of Murdama hornfels. BAJ-6-63.4 (RASS no. 208465)*

Figure 7.--*Photograph of aplitic quartz-porphyry dike, Stage 2) cutting more typical Baid al Jimalah porphyry dike with 5 mm phenocrysts of perthitic alkali feldspar, albite, and 2 mm phenocrysts of quartz and biotite. BAJ-6-108.2 (RASS no. 208471)*

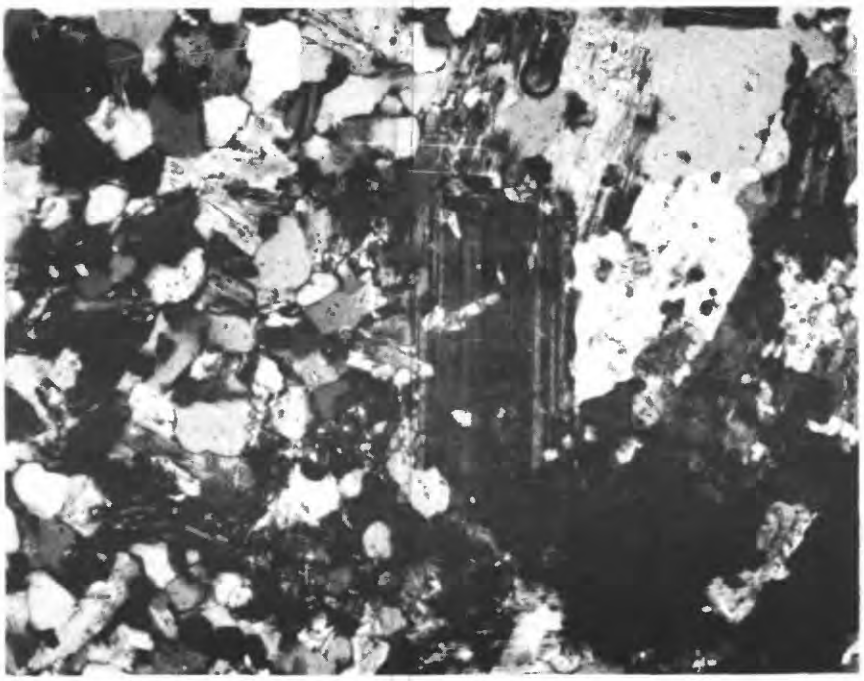

Figure 8.--*Photomicrograph of contact between main cupola and early dike. Fine-grained, aplitic groundmass at the apex of the main cupola (left half of photomicrograph) cuts off coarser-grained, hypidiomorphic groundmass of dike (right half of photomicrograph). BAJ-1-131.25 (RASS no. 208077)*

PETROGRAPHY OF ANALYZED ROCKS

Igneous rocks associated with mineral deposits commonly are altered, making it virtually impossible to obtain a fresh sample. Due to the presence of varying intensities of hydrothermal alteration in most samples, discussion of the chemical analyses will refer to the least altered sample, #889494, unless otherwise specified. Brief petrographic descriptions of each sample are given in the Appendix.

RESULTS AND DISCUSSION

The Baid al Jimalah granite is peraluminous (containing normative corundum) and highly differentiated. In terms of major elements (table 1), it is more highly differentiated than the average "specialized" granite of Tischendorf (1977). Tischendorf states that the most significant chemical characteristics that can be used to separate specialized granites associated with ore deposits of Sn, Li, Rb, Cs, Be, Nb, Ta, W, Mo and F from average granites are their contents of Ca, Ti, Si, and Mg. These four elements at Baid al Jimalah fall well within the range of the average specialized granite. The Baid al Jimalah granite has a higher differentiation index than the average specialized granite (93.08 versus 90.90).

Trace elements, however, tell a different story (table 2). Li, Rb, and Sn are well below the range of specialized granites, whereas Be and Mo are within the accepted range. This is in marked contrast to the Jabal as Silsilah tin deposit 110 km to the north, in which all the elements fall within the range of Tischendorf's

Table 1. --Major element analyses and CIPW norms for Baid al Jimalah granite.

[Major oxides and normative minerals in weight percent. D.I. is differentiation index of Thorton and Tuttle (1960). Fe_2O_3 and FeO calculated from total iron by assuming 2/3 of the iron is present as FeO. LOI is loss on ignition at 920° C. ND = no data]

Sample no.	889494[1]	893039[2]	893159[2]	893235[2]	Average specialized granite[3]	Average granite[4]
Drill hole no.	BAJ-3	BAJ-6	BAJ-6	BAJ-6		
depth (meters)	100.0	47.9-48.9	166.2-166.7	246.2-247.0		
Chemical Analyses						
SiO_2	75.32	76.40	75.32	77.75	74.30 ± 1.39	71.42 ± 1.41
Al_2O_3	12.44	11.27	11.76	10.76	14.15 ± 1.07	14.45 ± 0.23
Fe_2O_3	0.55	0.58	0.66	0.63	0.81 ± 0.47	1.32 ± 0.29
FeO	1.00	1.04	1.19	1.13	1.11 ± 0.47	1.79 ± 0.38
MgO	0.11	0.14	0.12	0.14	0.48 ± 0.56	0.82 ± 0.23
CaO	0.63	0.59	0.70	0.62	0.76 ± 0.41	1.91 ± 0.40
Na_2O	3.50	2.78	1.63	1.82	3.24 ± 0.61	3.47 ± 0.32
K_2O	4.66	4.31	5.64	4.77	4.75 ± 0.68	4.38 ± 0.52
TiO_2	0.08	0.09	0.10	0.10	0.16 ± 0.10	0.34 ± 0.08
P_2O_5	0.02	0.02	0.02	0.02	ND	ND
MnO	0.02	0.06	0.08	0.04	0.05 ± 0.04	0.06 ± 0.03
ZrO_2	0.02	0.02	0.02	0.02	ND	ND
CO_2	0.24	0.52	0.47	0.37	ND	ND
F	0.26	0.28	0.34	0.37	0.37 ± 0.15	0.08
S (total)	0.05	0.15	0.42	0.20	ND	ND
LOI	0.74	1.11	1.25	1.00	ND	ND
Total	99.64	99.36	99.68	99.74	100.14	100.04
CIPW norms						
Q	35.40	42.35	42.53	47.32	35.42	28.69
C	0.55	1.02	1.78	1.54	3.16	0.79
Z	0.03	0.03	0.03	0.03	ND	ND
Or	27.79	25.88	33.84	28.53	28.06	25.86
Ab	29.89	23.90	14.00	15.58	27.42	29.35
An	3.02	2.84	3.39	2.98	1.40	8.79
En	0.28	0.35	0.30	0.35	1.19	2.03
Fs	1.29	1.42	1.64	1.49	1.20	1.75
Mt	0.81	0.85	0.97	0.92	1.18	1.92
Il	0.15	0.17	0.19	0.19	0.31	0.65
Ap	0.05	0.05	0.05	0.05	ND	ND
Total	99.25	98.87	98.73	98.99	99.34	99.83
D.I.	93.08	92.14	90.37	91.43	90.90	83.90

[1] Weakly altered
[2] Moderately altered
[3] Tischendorf (1977)
[4] Krauskopf (1967)

Table 2. -- Trace element analyses for Baid al Jimalah granite.

[In parts per million. (1) Analyzed by 6-step semi-quantitative emission spectrography (2) Analyzed by ICP (3) Analyzed by energy dispersive X-ray fluorescence (4) Analyzed by delayed neutron counting ND = no data.]

Sample no.		889494[1]	893039[2]	893159[2]	893235[2]	Average specialized granite[3]	Average granite[4]
Drill hole no.		BAJ-3	BAJ-6	BAJ-6	BAJ-6		
depth (meters)		100.0	47.9-48.9	166.2-166.7	246.2-247.2		
Ag	(1)	<0.5	<0.5	<0.5	5	ND	0.04
As	(1)	<1000	<1000	1500	<1000	ND	1.5
B	(1)	<20	<20	<20	<20	ND	15
Ba	(3)	105	127	149	127	ND	250
Be	(2)	12	8	5	5	13 ± 6	5
Bi	(1)	<10	<10	15	150	ND	0.18
Cd	(1)	<50	<50	<50	<50	ND	0.2
Co	(3)	0.896	0.940	1.07	1.20	ND	1
Cr	(1)	1.5	3	2	1.5	ND	4
Cs	(3)	8.45	5.12	7.38	7.74	ND	5
Cu	(1)	20	30	30	30	ND	10
Hf	(3)	6.92	6.04	6.89	6.28	ND	4
Li	(2)	50	59	43	52	400 ± 200	30
Mo	(2)	6	2	5	4	4 ± 2	2
Nb	(3)	52	29	34	29	ND	20
Ni	(1)	<3	<3	<3	<3	ND	0.5
Pb	(1)	30	30	70	150	ND	20
Pd	(1)	<2	<2	<2	<2	ND	<0.05
Pt	(1)	<50	<50	<50	<50	ND	<0.05
Rb	(3)	316	363	251	291	550 ± 200	150
Sb	(3)	0.97	1.83	4.76	4.06	ND	0.2
Sc	(3)	2.26	1.94	2.48	2.67	ND	5
Sn	(1)	<10	15	15	15	40 ± 20	3
Sr	(3)	25	16	28	18	ND	285
Ta	(3)	8.11	5.02	5.60	5.04	ND	ND
Te	(1)	<2000	<2000	<2000	<2000	ND	<0.05
Th	(4)	35.2	24.4	29.6	28.9	ND	17
U	(4)	13.3	11.8	11.3	10.3	ND	4.8
V	(1)	<4	<4	<4	<4	ND	20
W	(2)	<20	74	48	310	7 ± 3	2
Y	(3)	86	64	59	63	ND	40
Zn	(1)	<300	<300	<300	<300	ND	40

[1] Weakly altered
[2] Moderately altered
[3] Tischendorf (1977)
[4] Krauskopf (1967)

Table 3. --Rare-earth element analyses for Baid al Jimalah. [In parts per million. Analyzed by energy dispersive X-ray fluorescence.]

Sample no.	889494	893039	893159	893235
Drill hole no.	BAJ-3	BAJ-6	BAJ-6	BAJ-6
depth (meters)	100.0	47.9-48.9	166.2-166.7	246.2-247.2
La	33.9	34.9	40.3	41.6
Ce	78.4	73.0	89.1	84.5
Nd	40.9	37.8	45.6	42.6
Sm	11.4	9.8	11.6	10.7
Eu	0.343	0.362	0.416	0.490
Gd	13.19	10.25	12.15	12.11
Tb	2.32	1.73	2.08	1.98
Dy	16.17	11.44	14.48	12.96
Tm	1.73	1.14	1.52	1.27
Yb	11.5	7.5	9.4	8.2
Lu	1.75	1.20	1.43	1.31

specialized granites. Although Baid al Jimalah and Jabal as Silsiah have the same age within the confidence limits of the techniques used (569±16 Ma versus 587±8 Ma) and both belong to the Abanat igneous suite (Cole and Hedge, 1986 and Du Bray, 1984), the latter deposit is associated with even more highly differentiated intrusive rocks than that of Baid al Jimalah (Du Bray, 1984; table 1, p. 19).

The rare-earth element patterns of rocks from Baid al Jimalah and Jabal as Silsilah (table 3 and fig. 9) support the hypothesis that Baid al Jimalah is the less differentiated of the two. Eu/Eu^* values are about one order of magnitude higher for Baid al Jimalah granite than for Fawwarah granite, with values for Baid al Jimalah at about 0.103 and values for Jabal as Silsilah between 0.005 and 0.075. The use of the ratio, Eu/Eu^*, is a method of quantifying Eu anomalies (Buma and others, 1971). Eu/Eu^* indicates the ratio of the measured Eu value to that expected by interpolation of measured values for Sm and Gd on chondrite-normalized diagrams. Values approaching 1.0 indicate the absence of an Eu anomaly, whereas values <0.10 are indicative of exceptionally large Eu anomalies. The existence of Eu anomalies in granitic rocks is generally attributed to feldspar fractionation (Buma and others, 1971). Feldspar fractionation is frequently invoked because Ca-bearing plagioclase and early-formed alkali feldspar are the only common rock-forming minerals that preferentially incorporate Eu.

The fact that the REE chondrite-normalized plots from the Baid al Jimalah granite analyses (fig. 9) are virtually identical to each other strongly imples that the granite represents a single intrusion of a chemically homogeneous magma.

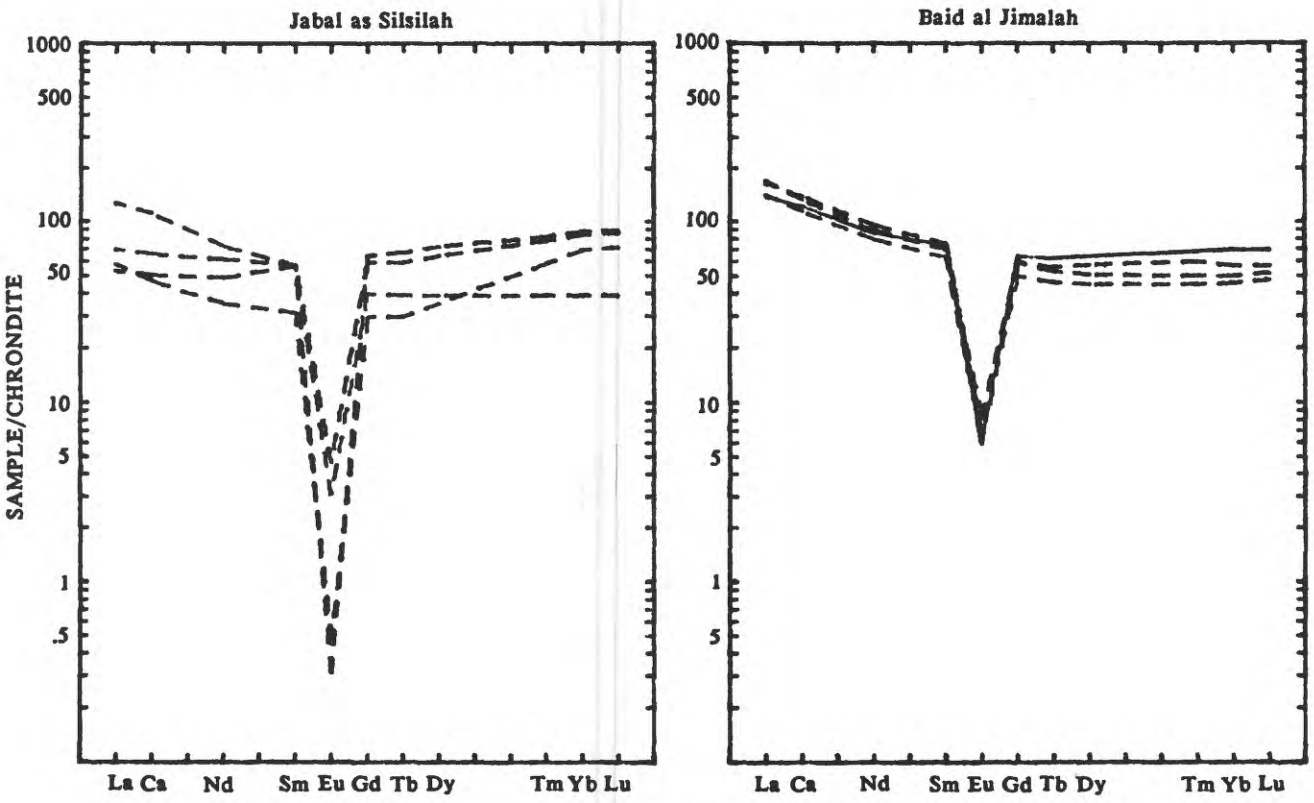

Figure 9.--*Chondrite-normalized rare-earth element diagram for Baid al Jimalah granite and Jabal as Silsiah. (from Stuckless and others, 1985).*

The differences in degree of differentiation are best seen in a ternary plot of Rb-Sr-Ba (fig. 10). Values for Baid al Jimalah, Jabal as Silsilah, Jabal al Gaharra and the Henderson molybdenum deposit in Colorado, USA are shown. Jabal al Gaharra and Henderson plot very close to the Rb corner of fig. 10, whereas Fawwarah granite extends toward the Ba corner, along the granite differentiation trend. Baid al Jimalah granite plots farther down this trend, toward less-differentiated rocks, but forms a distinct field, with no overlap with any of the other rocks plotted.

Figure 11 is a ternary plot of Rb-K/100-Sr. Both Henderson and Jabal al Gaharrah plot with the most highly differentiated rocks at Jabal as Silsilah, whereas the Baid al Jimalah granite plots with the earlier phases of the Fawwarah granite.

The effects of alteration on the chemical analyses of Baid al Jimalah granite are readily apparent in the ternary diagram of normative quartz-albite-orthoclase (fig. 12). Sample no. 889494 (the least altered) plots almost exactly on the granite minimum for 500 bars. The other three samples plot well above the cotectic, with samples nos. 893159 and 893235 outside of the field for 571 granites plotted by Tuttle and Bowen (1958). This shift is due to the conversion of the Na-bearing, alkali feldspars to quartz and muscovite during greisenization. Assuming that the weak alteration in sample no. 889494 has not significantly affected the whole rock chemical composition, we see that the Baid al Jimalah granite plots closer to the quartz corner of the diagram than samples from Jabal as Silsilah.

Data from Henderson and Jabal al Gaharrah are also plotted in figure 12 for comparative purposes. It is interesting to note that Jabal al Gaharrah, a tin deposit, plots with the rocks from Jabal as Silsilah, also a tin deposit; whereas the relatively unaltered sample from Baid al Jimalah (a tungsten deposit with accessory molybdenum) plots very close to the Henderson rocks (a molybdenum deposit with accessory tungsten). This difference probably represents two real subgroups within ore deposits associated with specialized granites.

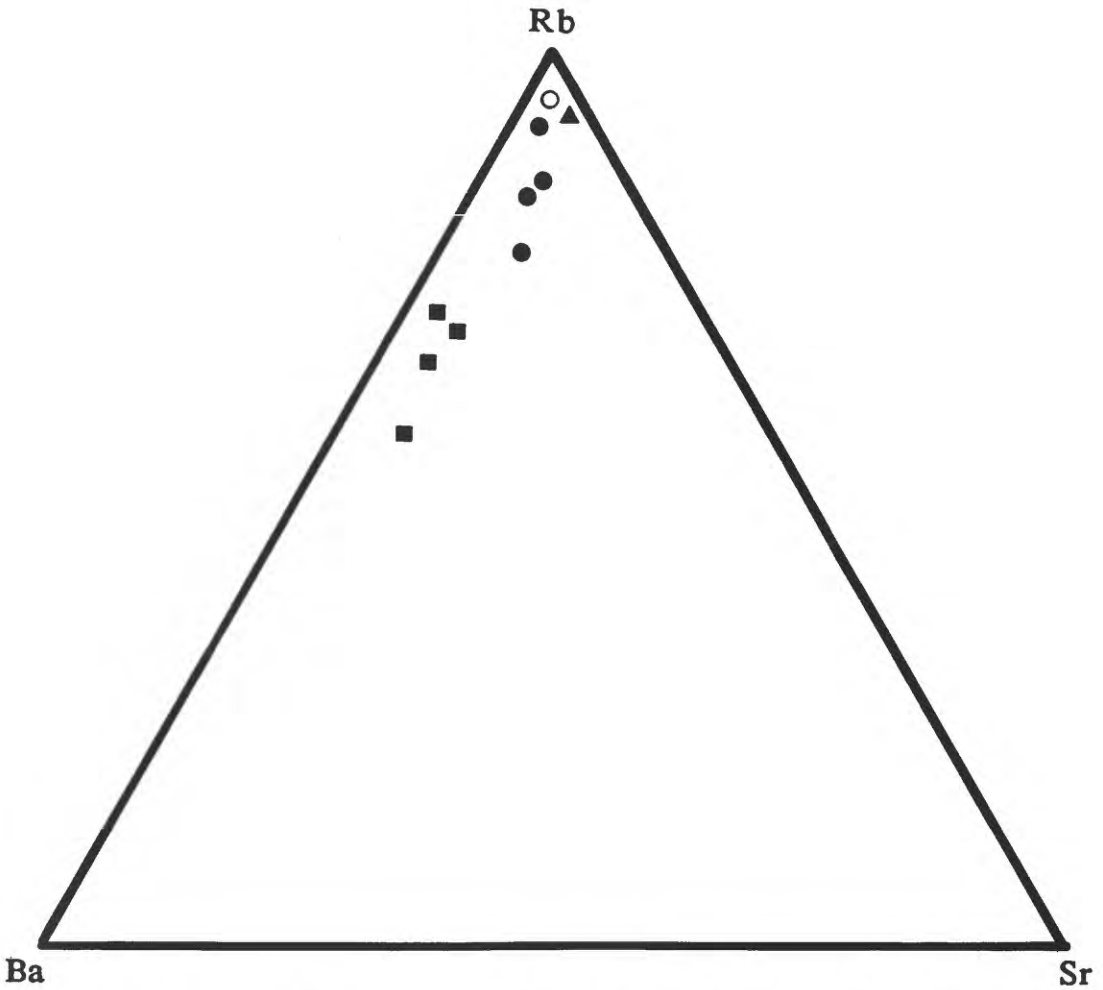

Figure 10.--*Ternary diagram of whole rock Rb-Sr-Ba analyses for Baid al Jimalah granite (■), Fawwarah granite from Jabal as Silsilah (●), Jabal al Gaharra granite (○), and intrusive rocks from the Henderson molybdenum deposit (▲). (Data from J. Stuckless (written commun., 1985), Du Bray (1984), Elliott (1980), and White and others (1981), respectively).*

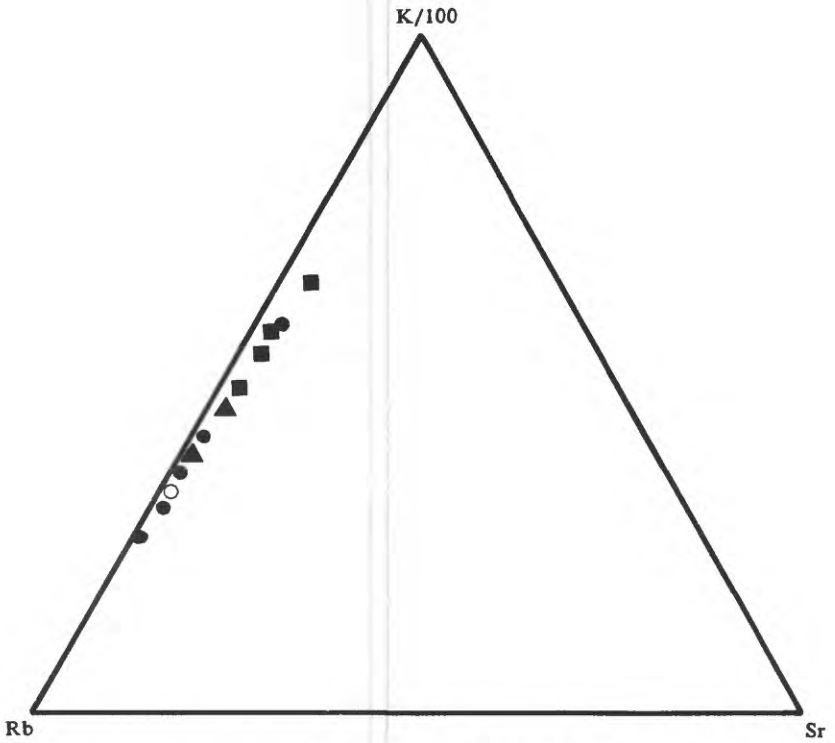

Figure 11.--*Ternary diagram of whole rock Rb-K/100-Sr analyses for Baid al Jimalah granite (■), Fawwarah granite from Jabal as Silsilah (●), Jabal al Gaharra granite (○), and intrusive rocks from the Henderson molybdenum deposit (▲). (Data from J. Stuckless (written commun. 1985), Du Bray (1984), Elliott (1980), and White and others (1981), respectively.)*

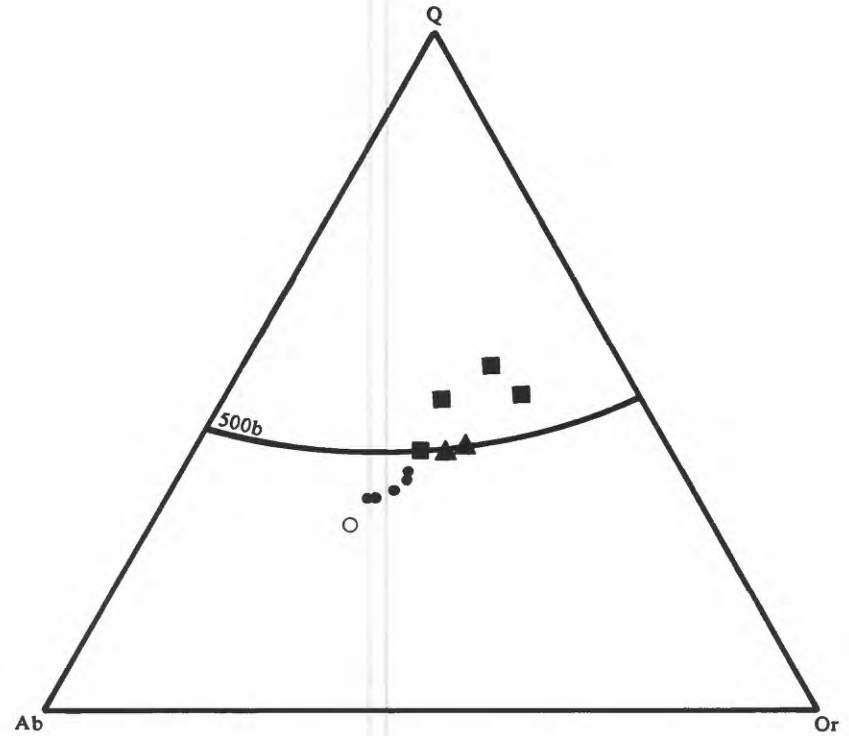

Figure 12.--*Ternary normative quartz-albite-orthoclase diagram for Baid al Jimalah granite (■), Fawwarah granite from Jabal as Silsilah (●), Jabal al Gaharra granite (○), and intrusive rocks from the Henderson molybdenum deposit (▲). (Data from J. Stuckless (written commun., 1985), Du Bray (1984), Elliott (1980), and White and others (1981), respectively.)*

PARAGENESIS AND MINERALOGY OF VEINS AND ALTERATION

INTRODUCTION

Paragenesis and mineralogy were studied by core-logging, detailed mapping of trenches, and laboratory studies of hand samples, thin sections, and polished sections. All eleven trenches at Baid al Jimalah West, plus the main ancient trench at Baid al Jimalah East, were mapped at a scale of 1:200 in March, 1984 in order to document the samples taken for study. Additional samples were collected on radial traverses as much as two kilometers from Baid al Jimalah West to obtain samples beyond the known limits of mineralization and alteration. The six diamond drill holes drilled by Riofinex Ltd., totaling 1116 meters, were logged and sampled for this study. A total of 305 samples were collected from the surface, trenches, and drill core and studied in the laboratory. Samples for fluid inclusion, isotopic, and detailed petrographic study were selected from this suite. The diamond drill core samples proved to be far superior to the trench samples because of the lack of weathering effects.

The vein paragenesis at Baid al Jimalah West is summarized in figure 13. This form of presentation is especially well-suited to deposits in which the history of mineralization and alteration is recorded in many crosscutting veins, each vein belonging to a specific generation. Both quality and quantity of information gathered is shown and each stage of mineralization is listed on both the horizontal and vertical axes. Data are recorded only in the boxes within the area defined by the first column, first row; last column, last row; and first column, last row. Relative age between two veins is recorded in the box corresponding to the intersection of the appropriate row and column and is denoted by an arrow pointing to the older vein. "C" denotes a crosscutting relationship, and "O" denotes an offsetting relationship. The numbers in parentheses give the total number of observations. For example, the box formed by the intersection of the Stage 3 row and Stage 1 column indicates that eight observations were made of Stage 3 veins cutting Stage 1 veins in Murdama; seven observations were made of Stage 3 veins offsetting Stage one veins in Murdama; one observation was made of a Stage 3 vein offsetting a Stage 1 vein in the granite.

Vein-offsets are much more reliable than mere crosscutting relationships because vein-offsets are generally unambiguous. This type of diagram also allows one to tell at a glance if there are any apparent violations of the paragenesis. If all arrows point upward, as is the case in figure 13, then there are no violations. An apparent violation of the paragenesis can be due to one of three reasons: the first is that the vein was assigned to the wrong stage, the second is that the age-relation was incorrectly interpreted, and the third is that there are more stages than originally hypothesized. The third reason is especially significant for the recognition of ore deposits where more than one cycle of mineralization took place. For, example, in a system with an early, barren vein generation and a later, ore-bearing vein generation, if "early" barren veins cut "later", ore-bearing veins, we can infer that there must have been at least two cycles of mineralization, each associated with a different intrusion or hydrothermal pulse. Thus, high-grade deposits can form by multiple cycles of mineralization. Wallace, and others (1968) demonstrated that high-grade, stockwork-molybdenite (Climax-type) deposits result from multiple intrusions of granite porphyry and their associated pulses of hydrothermal mineralization affecting a single volume of rock and increasing the total grade within each pulse. Of special note is that

no apparent violations of the vein paragenesis were observed at Baid al Jimalah (all arrows point upward in figure 13). This is conclusive evidence that there was only one cycle of mineralization at Baid al Jimalah. Veins at Baid al Jimalah West include a pre-intrusion, metamorphic set and numerous intrusion-related varieties. The hypogene mineralization (fig. 14) at Baid al Jimalah West can be divided into three periods: (1) early stockwork veins and aplitic dikes; (2) greisen veins; and (3) late, barren veins. The first two periods can be further subdivided into distinct stages. The first period comrises two stages: (1) quartz - molybdenite stockwork veins; (2) aplite dikes and "vein-dikes". The second period comprises three stages: (3) early, feldspar-bearing, greisen veins; (4) main stage, feldspar-free greisen veins; (5) late greisen veins, with both feldspar and wolframite unstable and characterized by the presence of scheelite. No crosscutting relationships were observed to allow the determination of the relative ages of the late quartz fluorite veins and calcite veins. They are therefore combined into a single, final stage: (6).

	Meta-morphic veins	Stage 1	Stage 2	Stage 3	Stage 4	Stage 5	Stage 6
Meta-morphic veins	↑ O (3)						
Stage 1	↑ C (1) ↑ O (1)	↑ O (1)					
Stage 2	↑ C (2)	↑ C (3) ↑ C (1) (g)	↑ C (2)				
Stage 3	↑ C (14) ↑ O (4)	↑ C (8) ↑ O (7) ↑ O (1) (g)	↑ C (4) ↑ C (1) (g)	↑ O (2)			
Stage 4	↑ C (1)			↑ C (1) (g) ↑ C (1)			
Stage 5				↑ C (4) ↑ O (2)	↑ C (2)		
Stage 6		↑ C (1)		↑ C (2)			↑ O (1)

Figure 13.--*Paragenesis diagram showing cross-cutting vein data for Baid al Jimalah West. "C" and "O" signify cross-cutting and off-setting relationship. Arrows point to older veins. "(g)" denotes veins in granite (all others are in Murdama). Numbers in parentheses refer to number of observations. See text for discussion. This diagram does not include replacement textural relationships by greisen Stages 4 and 5 of earlier veins and mineralization.*

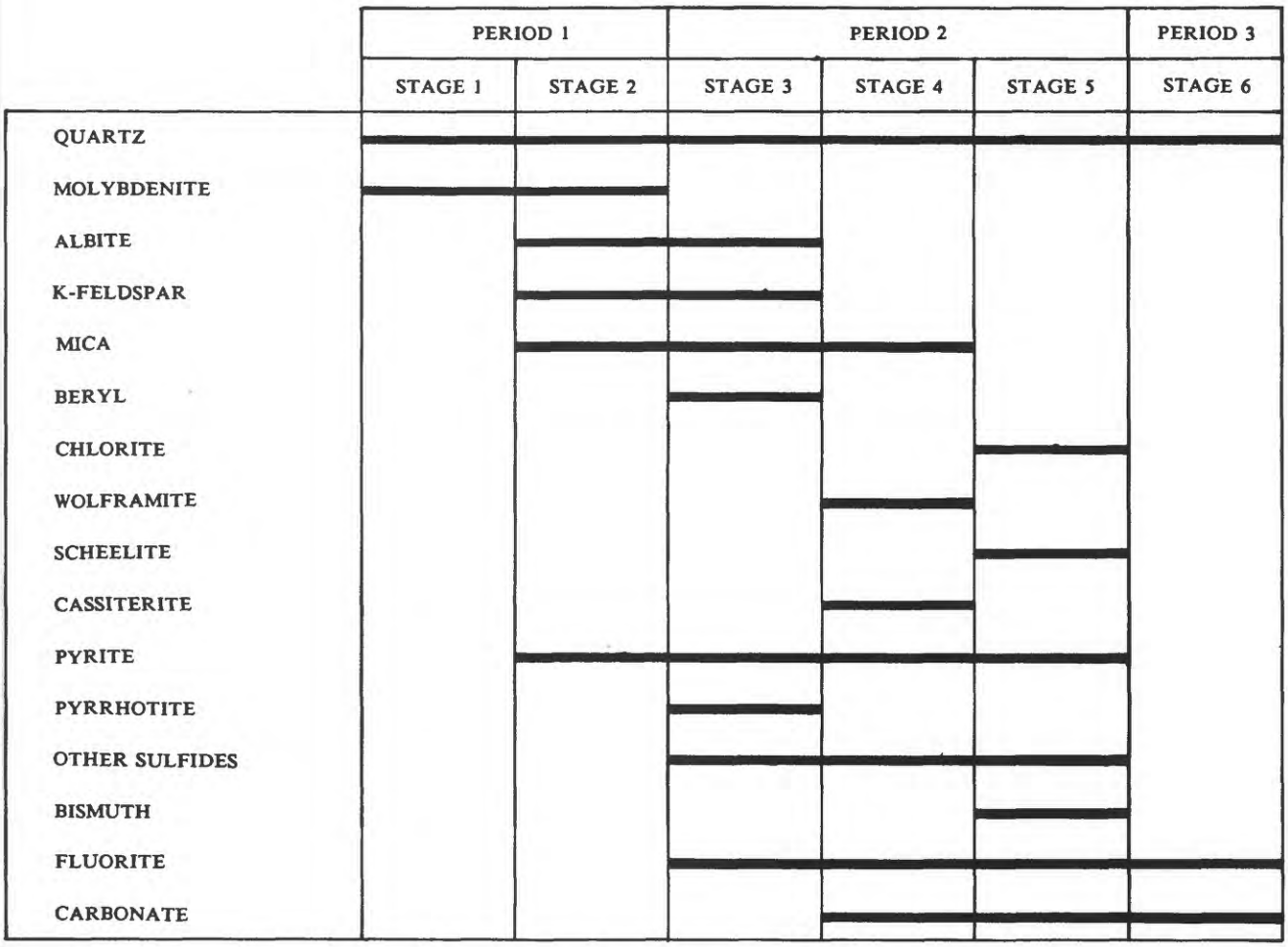

Figure 14.--*Paragenesis diagram for mineralization at Baid al Jimalah East and West. See text for explanation.*

PRE-INTRUSION, METAMORPHIC VEINS

The pre-intrusion, metamorphic veins, which are only found in the Murdama, range in width from less than one millimeter to a maximum of one centimeter. The most distinctive characteristic of these veins is that they are irregular replacement veins with indistinct boundaries and may appear as tension gash fillings (fig. 15). They are largely composed of sutured intergrowths of quartz with minor biotite, but may also contain pyrrhotite, pyrite, chlorite, sericite, and a carbonate. It is probable that much of the observed biotite in these veins was formed during the formation of the hornfels associated with the intrusion of the Baid al Jimalah stock.

PERIOD 1

Stage 1, Quartz - molybdenite veins

The earliest mineralization associated with the intrusion of the Baid al Jimalah stock is represented by 5-10 mm quartz veins (fig. 16); characterized by small plates of molybdenite intergrown with sutured intergrowths of quartz. Traces of pyrite may also be present. Carbonate and muscovite commonly occur along microfractures and grain boundaries. It is likely that most, if not all, of the muscovite and carbonate formed during Stages 4 and 5 and do not properly belong to Stage 1. No alteration envelopes are evident around these veins. Despite the lack of symmetrical banding or other positive criteria, the distinct contact between these veins and the wall rock indicate that they formed by open-space filling rather than by replacement. These veins commonly exhibit boudinage and appear to have been plastically deformed (figs. 17 and 18).

Stage 2, Aplite dikes and "vein dikes"

Aplite dikes, generally 1 to 10 cm wide, commonly cut Stage 1 veins. The aplite is slightly porphyritic, with only quartz phenocrysts observed. The groundmass ranges from 0.2 to 1 mm and comprises greater than 95 percent of the rock; it is not truly aplitic in texture, but rather hypidiomorphic-granular, and is composed of ca. 40 percent perthitic, alkali feldspar, ca. 35 percent quartz, and ca. 20 percent albite. Both feldspars typically exhibit replacement by muscovite (ca. 5 percent) and manganosiderite (<1 percent). These dikes are seen always to cut more typical Baid al Jimalah porphyry, the latter being characterized by large feldspar phenocrysts (fig. 7), and they also cut Stage 1 veins (fig. 19). The most striking feature of these aplite dikes is that they may have borders of hydrothermal quartz plus trace molybdenite. These borders are Stage 1 quartz, and have no apparent alteration envelopes (figs. 20 and 21). Such features, with characteristics of both igneous dikes and hydrothermal veins, have been found in other deposits where hydrothermal mineralization is closely associated in time and space with the intrusion and crystallization of a granitic magma, generally within 25 meters of an igneous contact, and have been called "vein-dikes" by White, and others (1981). It is therefore more correct to consider Stage 1 and 2 mineralization as part of the same event. Stage 2 aplite dikes, as well as vein-dikes, commonly show boudinage and disruption with little or no evidence of crosscutting structures (fig. 22).

It is the author's opinion that the veins and dikes of Stages 1 and 2 form a stockwork of randomly oriented structures, although this can not be conclusively demonstrated. Lofts (1982) mentions that oriented core logging of diamond drill hole BAJ-6 showed that there was only one dominant vein set that strikes from S. 76° W. to N. 22° E. and dips from 60° southwest to 75° northeast. He also states that minor veins (<5mm) with strikes and dips outside this range are randomly oriented; a feature that is also apparent in outcrop (fig. 26). It is probable that these randomly oriented veins include all of those in Stages 1 and 2. The most compelling evidence for random orientation in structures belonging to Stages 1 and 2 can be seen in the core. Inasmuch as most of the greisen veins (Stages 3 and 4) have the dominant WNW strike direction, it is evident that the earlier structures commonly have a very different orientation from the greisen veins (figs. 15, 16, 17, 18, 20, 21, and 22).

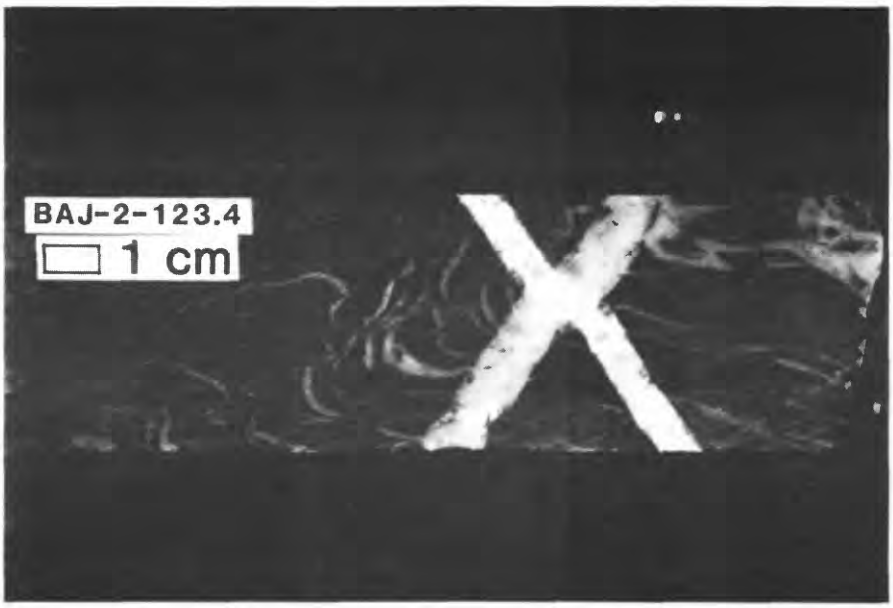

Figure 15.--*Photograph of metamorphic quartz in tension gashes cut by Stage 3 veins. BAJ-2-123.4 (RASS no. 208413)*

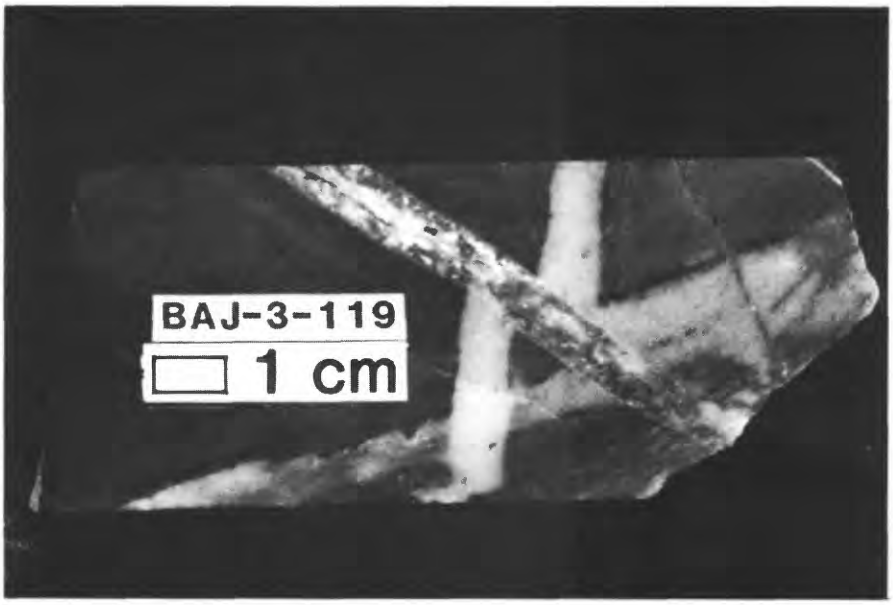

Figure 16.--*Photograph of a Stage 3 vein offsetting a Stage 1 vein, which, in turn cuts a metamorphic vein. The irregularly-bounded metamorphic vein is composed of quartz, sericite, and pyrite. The Stage 1 vein is composed of quartz plus <1% molybdenite. The Stage 3 vein has a symmetrical selvage of muscovite on its border, with a center composed of quartz, potassium feldspar, fluorite, pyrite and sphalerite. BAJ-3-119 (RASS no. 208418)*

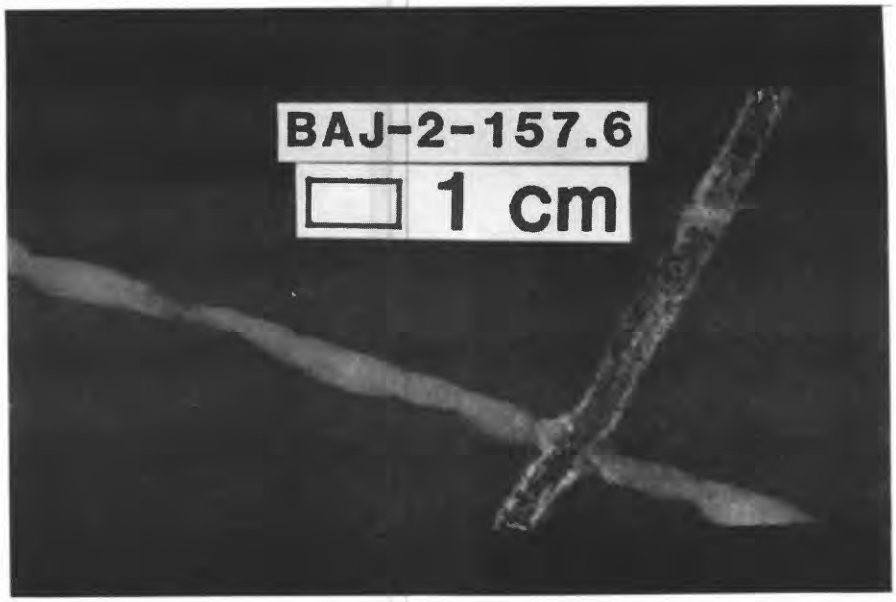

Figure 17.--*Photograph of a Stage 1, quartz - molybdenite vein, showing boudinage, cut by Stage 3 quartz - muscovite - potassium feldspar - pyrrhotite vein. BAJ-3-157.6 (RASS no. 208414)*

Figure 18.--*Photograph of a Stage 1, quartz - molybdenite vein dilationally offset by Stage 3, quartz - potassium feldspar - muscovite - fluorite vein. BAJ-2-176 (RASS no. 208415)*

Figure 19.--*Photograph of an irregular aplite dike (Stage 2) cutting Stage 1 quartz - molybdenite vein. BAJ-1-83.7 (RASS no. 208052)*

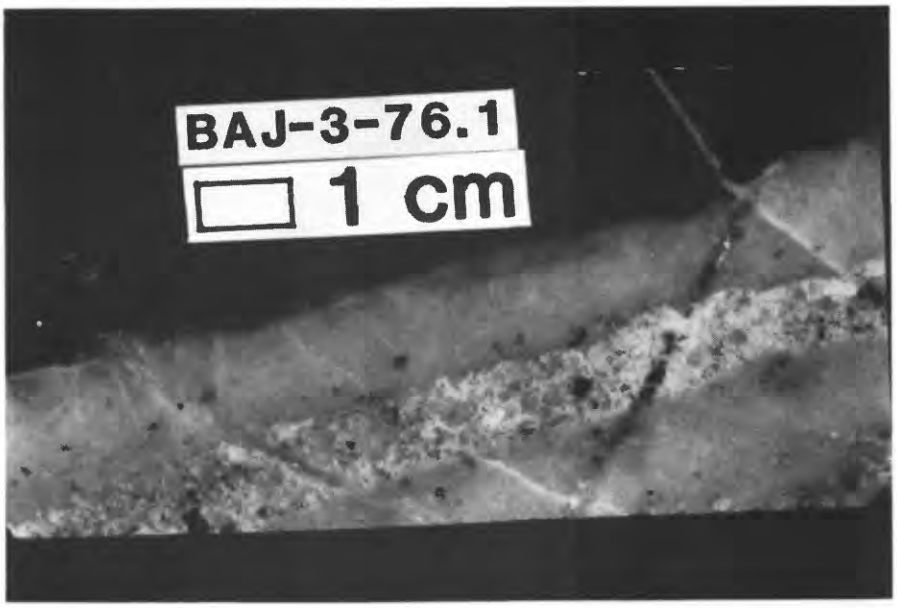

Figure 20.--*Photograph of a vein-dike with quartz plus trace molybdenite symmetrically arranged on either side of an aplitic quartz porphyry center (Stage 2). The vein-dike is cut by a 1 mm aplite dike (also Stage 2), and both are cut by a 2 mm, quartz - white mica Stage 3 vein. BAJ-3-76.1 (RASS no. 208210)*

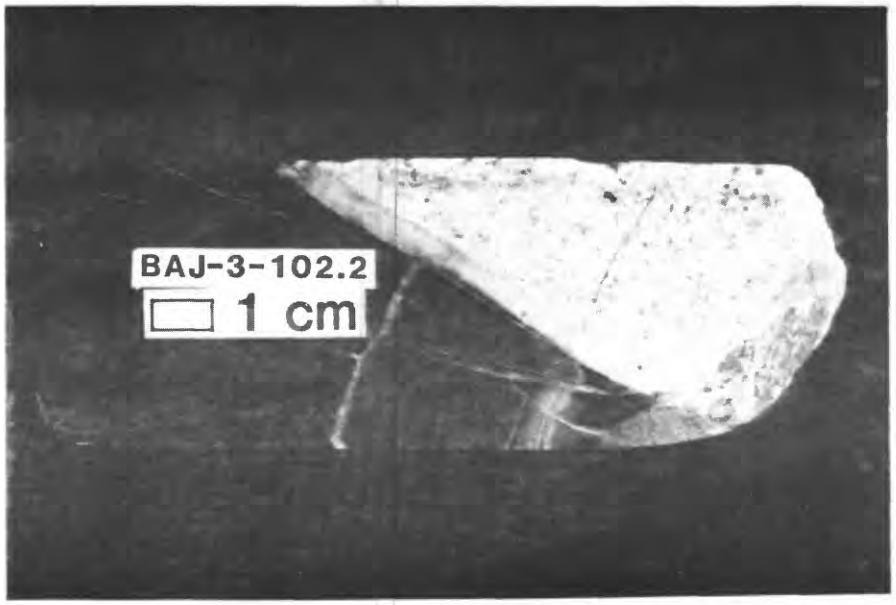

Figure 21.--*Photograph of a vein-dike (Stage 2), similar to the one shown in figure 20, but with a narrow quartz border and a wide, aplitic center. BAJ-3-102.2 (RASS no. 208420)*

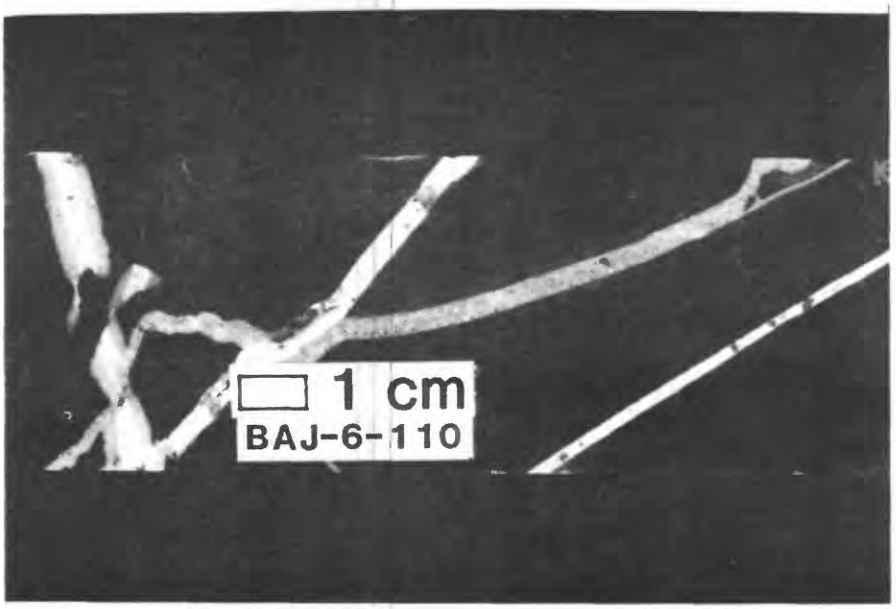

Figure 22.--*Photograph of a vein-dike (Stage 2) (on left), showing apparently fracture-free disruption. It is cut by an aplite dike (Stage 2), exibiting boudinage, and, in turn, is cut by a feldspar - fluorite - quartz - muscovite Stage 3 vein. BAJ-6-110 (RASS no. 208472)*

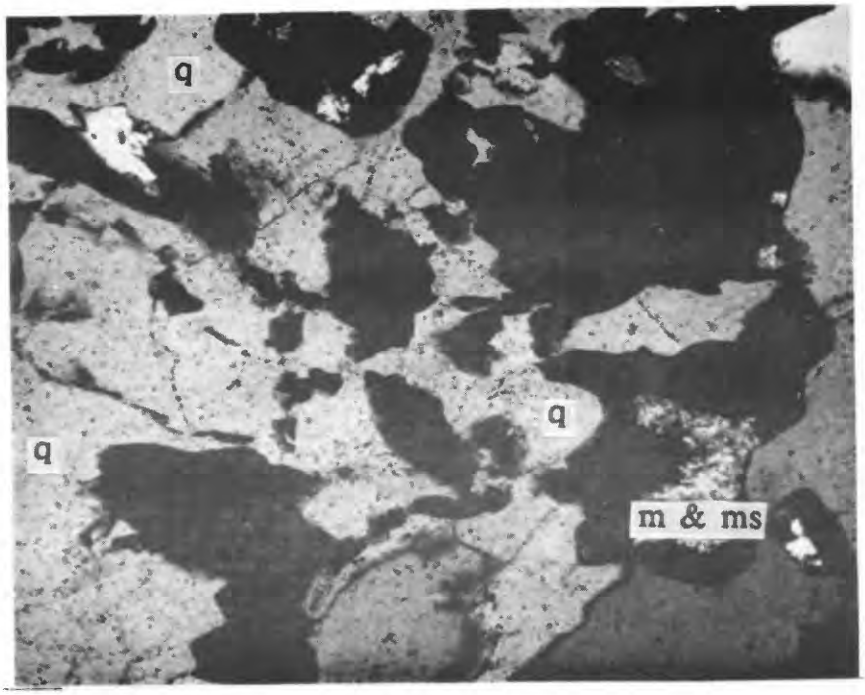

Figure 23.--*Photomicrograph of a Stage 3 vein, showing replacement of potassium feldspar (at extinction) by quartz (q), muscovite (m), and manganosiderite (ms). BAJ-2-116.3 (RASS no. 208188)*

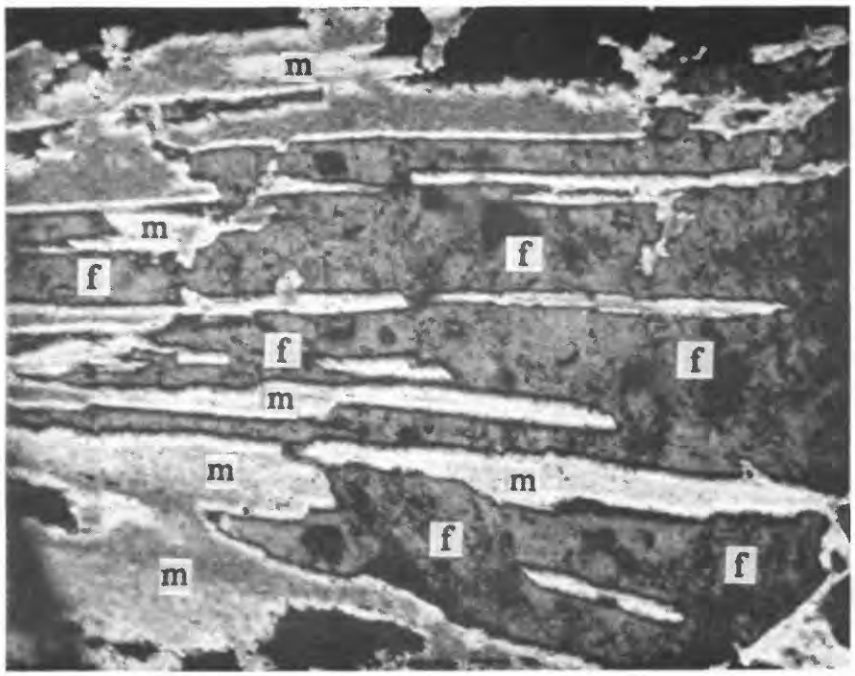

Figure 24.--*Photomicrograph of a Stage 3 vein with muscovite (m) growing inward from wall-rock contact and being succeeded and replaced by potassium feldspar (f). BAJ-1-48.5 (RASS no. 208029)*

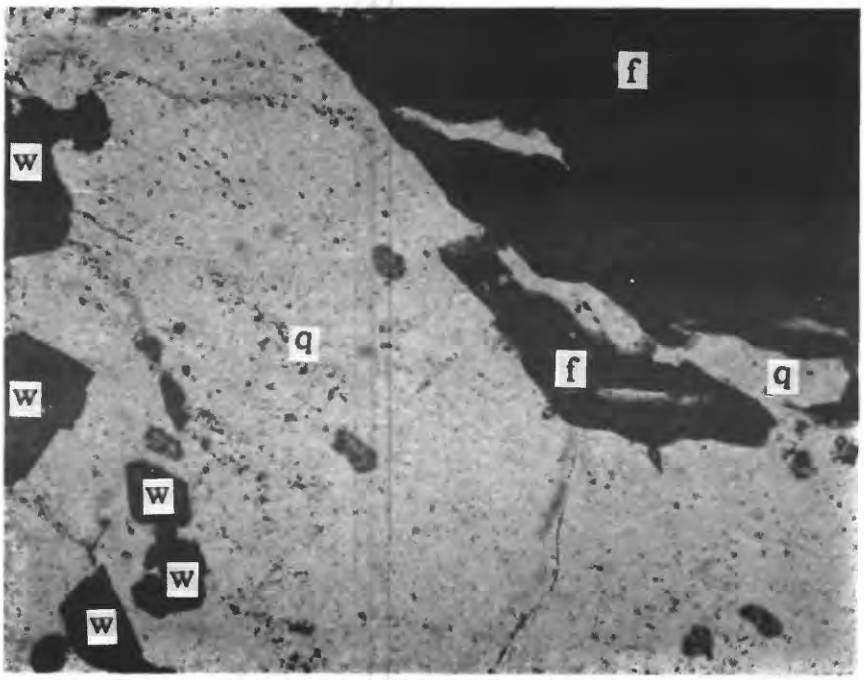

Figure 25.--*Photomicrograph of a different part of the same vein shown in figure 23, showing wolframite (w) (black and subhedral) in area where most of the potassium feldspar (f) (ragged and at extinction) has been replaced by quartz (q). BAJ-2-116.3 (RASS no. 208188)*

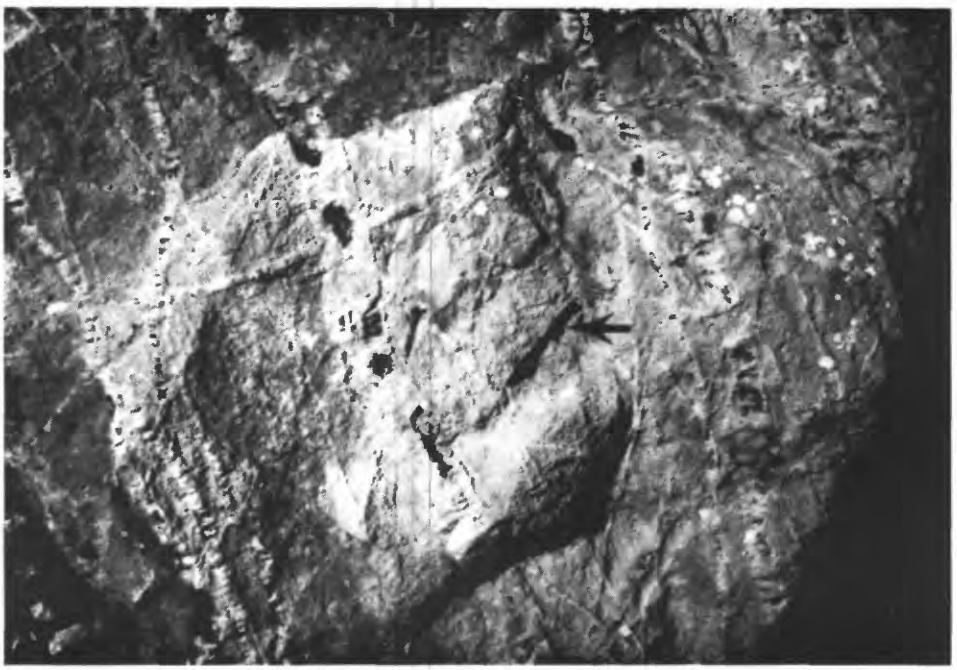

Figure 26.--*Photograph of boulder exposed during excavation of one of the trenches. Large, quartz-rich veins are sub-parallel, vuggy and belong to Stages 4 and 5. Note black ball-point pen included for scale.*

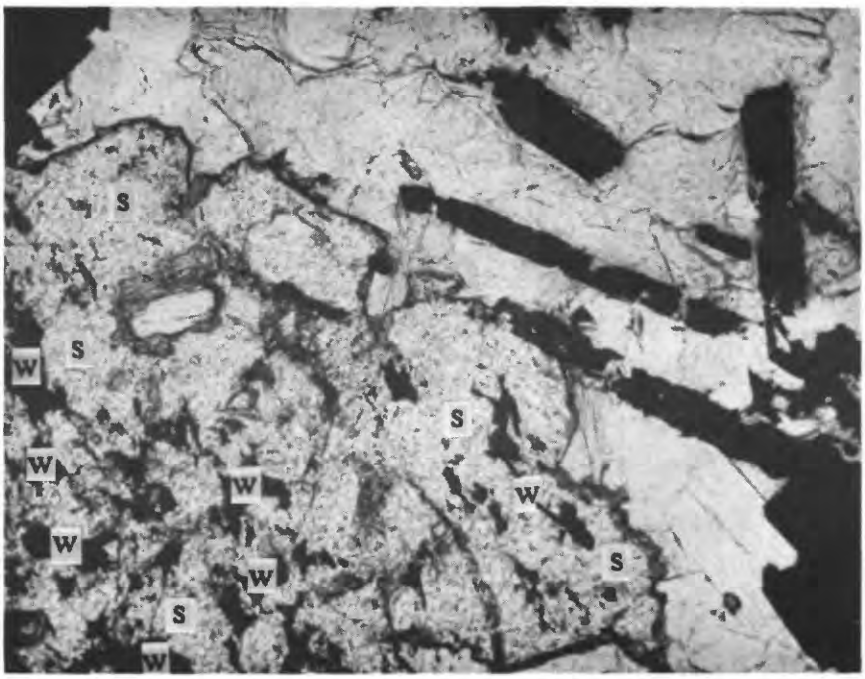

Figure 27.--*Photomicrograph of scheelite (s) with remnant wolframite (w) in the interior of the crystal. BAJ-3-115.6 (RASS no. 208214)*

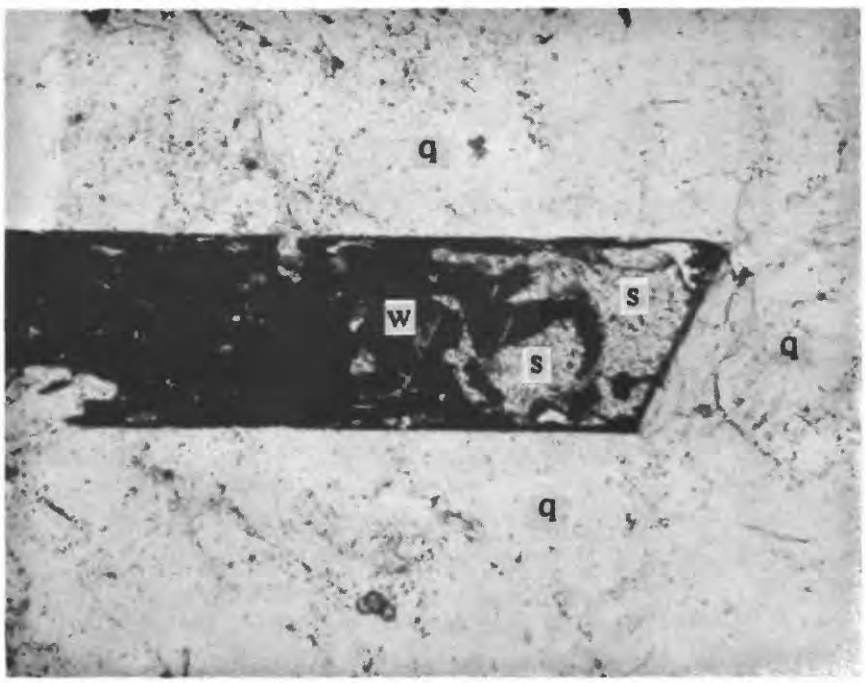

Figure 28.--*Photomicrograph of euhedral wolframite crystal (w) in quartz (q) with pseudomorphic replacement by scheelite (s). BAJ-6-191 (RASS no. 208479)*

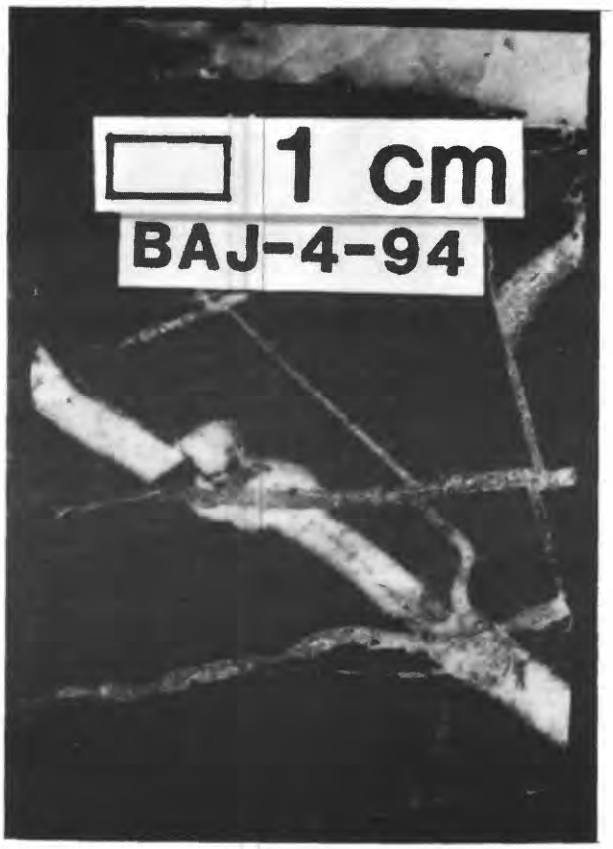

Figure 29.--*Calcite veins (horizontal) cut Stage 3 quartz, feldspar and white mica vein. BAJ-4-94 (RASS no. 208437)*

PERIOD 2

Stage 3, Early greisen veins

Stage 3 veins are the most abundant in the deposit at Baid al Jimalah West, but carry little in the way of ore minerals (wolframite and cassiterite). The veins range in thickness from 1 mm to 10 cm, but most are less than 2 cm. They are characterized by open-space filling and the presence of feldspar. Where the veins cut Murdama rocks, symmetrically arranged sheaves of white mica selvages are common. Greisen envelopes in the wall rocks, if present, are small. Biotite-rich Murdama hornfels is generally found at the wall rock - vein contact. Primary minerals in the veins are (in decreasing order of abundance) quartz, perthitic alkali feldspar, muscovite, manganosiderite (much of which may be secondary), fluorite, pyrite, wolframite, chalcopyrite, sphalerite, cassiterite, pyrrhotite, and beryl. Secondary minerals include quartz, muscovite, manganosiderite, sericite, chlorite, clay, and iron oxide.

These veins typically show complex replacement relationships among the various minerals and are clearly transitional to Stage 4 veins. Alkali feldspar commonly shows various degrees of replacement by quartz, muscovite and manganosiderite (fig. 23). Also evident in many symmetrical muscovite veins is that, after initial precipitation of muscovite, the muscovite was succeeded by feldspar and even replaced by it, even though the feldspar was, in turn, replaced by muscovite (fig. 24). Muscovite is also replaced by quartz, but not to the extent that feldspar is. Wolframite and cassiterite generally occur only where feldspar is absent (fig. 25).

Stages 4 & 5, Main stage and late greisen veins

Stage 4 mineralization contains the bulk of wolframite, cassiterite and other ore minerals at Baid al Jimalah West. Most of the prominent veins visible on the surface belong to this stage, as does most of the hydrothermal alteration of the granite and Murdama rocks. Individual veins can be as much as 30 cm wide, but most are in the range of 1-10 cm and are commonly vuggy (fig. 26). They generally occur in parallel swarms, creating composite alteration envelopes on the scale of tens of meters. Vein minerals (in decreasing order of abundance) are: quartz, muscovite, fluorite, manganosiderite, pyrite, wolframite, scheelite, chalcopyrite, cassiterite, sphalerite, arsenopyrite, galena, bornite, bismuthinite, and chlorite. Two common greisen minerals, topaz and tourmaline, are scarce. Quartz, scheelite, fluorite, manganosiderite, and chlorite form a distinct sub-assemblage, are distinctly later than the other minerals and are given the status of a separate stage, 5. Wolframite appears to be stable when enclosed in quartz, but where it is close to vugs or in contact with the Stage 5 assemblage, it is replaced by scheelite. In fact, most of the scheelite observed can clearly be seen to be forming at the expense of wolframite (figs. 27 and 28).

Alteration envelopes can be large, but typically have relatively sharp boundaries with the country-rock. Most of the granite in the Baid al Jimalah stock shows weak greisenization, with some replacement of microcline and albite by sericite and a carbonate (probably manganosiderite). The primary biotite is generally unstable, even in the fresh rocks. Intense greisenization destroyed all original igneous texture except for some indistinct quartz phenocrysts. The change from weak to strong greisenization can occur over a space of less than one meter. As a Stage 4 greisen vein is approached, muscovite increases in abundance (as much as 25 percent) and grain size, but the percentage of quartz remains more or less constant. Closer to the vein(s), the percent of muscovite decreases as silification becomes the dominant process. The volume of quartz can be as much as 90 percent adjacent to the veins. Disseminated pyrite, chalcopyrite, sphalerite with chalcopyrite exsolution blebs, and un unknown, blue-gray opaque mineral occassionally occur in the alteration envelope close to the vein. Fluorite and manganosiderite each can be as much as 5 percent.

PERIOD 3

Stage 6, late quartz and carbonate veins

The last recognizable mineralizing event at Baid al Jimalah West formed minor calcite veins and veins with drusy and chalcedonic quartz$\pm$fluorite that crosscut all earlier veins (fig. 29).

Baid al Jimalah East

Three types of mineralization can be seen in the principal trench at Baid al Jimalah East. The first, and most dominant type, is limonite- and hematite-rich quartz, with sericite, clay, and some relict pyrite. Boyle and Howes (1983) also report galena, copper sulfides, and malachite, but these minerals were not observed during this study. The second type is composed entire of massive,

milky quartz. The third, and volumetrically most insignificant type, is composed of quartz stringers with trace amounts of cassiterite and apatite.

It is impossible to fit the veins of Baid al Jimalah East into the paragenetic sequence for Baid al Jimalah West, because of the lack of crosscutting relations. Moreover, it is impossible to state with absolute certainty that the veins of Baid al Jimalah East and of Baid al Jimalah West are genetically related. Nevertheless, the facts that the veins have the same strike as the main veins at Baid al Jimalah West and have as much as 235 ppm Sn (Boyle and Howes, 1983), plus the observed cassiterite, all suggest strongly that Baid al Jimalah East is part of the Baid al Jimalah West hydrothermal system. This conclusion is also supported by the fluid inclusion data.

DISCUSSION

The presence of aplite dikes cutting Stage 1 veins, as well as the presence of vein-dikes is the most compelling field evidence for the magmatic origin of hydrothermal deposits (White and others, 1981). Vein-dikes have characteristics of both igneous dikes and hydrothermal veins. They record the transition from predominantly igneous to predominantly hydrothermal processes, and are found close to igneous contacts. The presence of vein-dikes and many Stage 2 veins in drill core from BAJ-3 between 76 meters to the end of the hole at 182.5 meters suggests that the hole comes very close to the main stock, although only scattered porphyry dikes are encountered.

The boudinage and disruption of the veins and vein-dikes of Stages 1 and 2 are clearly associated with the intrusion of the 569 Ma Baid al Jimalah stock and can not be attributed to folding during the burial metamorphism of the Murdama at around 655 Ma. Because this deformation is not apparent in later veins, it is considered that the deformation was associated with the intrusion of the magma. Careful inspection of samples indicates that this deformation is similar to shear folding (gleitbretter), where the whole rock may be traversed by minutely spaced planes of relative movement. This type of deformation is probably important in the intrusion of most high level stocks, where evidence of stoping is usually limited, as it is at Baid al Jimalah, and because country rocks must accomodate the added volume.

Stages 3, 4, and 5 show a complex interplay between the evolving hydrothermal fluids, the wall rocks, and previously deposited minerals. Hydrothermal fluids of Stage 3 must have been near the muscovite-potassium feldspar stability boundary because Stage 3 veins that cut granite are dominated by the assemblage quartz + feldspar, whereas the characteristic muscovite selvage of those Stage 3 veins which cut Murdama hornfels, and the paucity of alteration envelopes around them, show that the host rock was buffering the K^+/H^+ in the hydrothermal fluids at first. During the mineralization of a single Stage 3 vein, the hydrothermal fluid became the K^+/H^+ buffer and potassium feldspar precipitated in the center of the veins, locally replacing the earlier-formed white mica. Subsequently, the hydrothermal fluids changed chemistry markedly and commenced Stage 4 mineralization, greisenizing the wall rocks and previously deposited minerals, especially Stage 3 feldspar. This was the main period of wolframite deposition. During Stage 5, the calcium-rich assemblage, quartz + scheelite + manganosiderite + fluorite became stable, and much of the wolframite

was replaced by scheelite. It is probable that much of the Ca^{2+} came from alteration of the wall rock, because none of the alteration minerals are calcium-bearing. Any released Ca^{2+} would immediately combine with F^- to form fluorite and with WO_4^{2-} to form scheelite.

The most important conclusion that can be drawn from this paragenetic study is that there was only one cycle of intrusion and mineralization at Baid al Jimalah. The fact that the paragenesis is so clear-cut, with no violations of the vein sequence, can allow unambiguous geological studies of the mineral deposit. It seems likely that no considerable tonnage will be found with grades greater than the mean grades of 0.117 percent WO_3 and 0.012 percent Sn (Lofts, 1982). This conclusion about the economic potential of Baid al Jimalah is supported by the fact that all the igneous rock appears to have come from the same stock and no evidence of multiple cycles of intrusion were seen.

FLUID INCLUSION STUDIES

INTRODUCTION

Thin sections from 131 samples were examined for suitability for fluid inclusion studies. Of these, 11 samples were chosen to make doubly-polished thick sections for fluid inclusion petrography, crushing, and heating/freezing studies. Data were obtained for all paragenetic stages except Stage 5 because no suitable inclusions were found in samples of that stage. A total of 152 homogenization and decrepitation temperatures were measured and a total of 91 salinities were determined. The measurements were made using a modified USGS gas-flow heating/freezing system manufactured by Fluid Inc. of Denver, Colorado, in conjunction with a Leitz SM-LUX-POL microscope. Instrumental precision is $\pm 0.1^{o}C$. The data are summarized in tables 4 and 5 and in figures 30 and 31.

Three catagories were used for classification of the fluid inclusions: Primary (P), Secondary (S), and Indeterminate (I). Each data point is classified according to this scheme in the heating and freezing data histograms (figs. 30 and 31). Primary fluid inclusions were identified on the basis of isolated occurrence or occurrence as a small, three-dimensional group. Secondary inclusions were identified on the basis of occurrence as planar groups. Some errors in classification were probably made, but the general consistency of the data indicates that this was not often the case. All samples had obviously late, secondary, low temperature, liquid-rich, aqueous fluid inclusions; some of these had no vapor bubble. The single-phase liquid inclusions were cooled to see if they nucleated a bubble that would indicate they were CO_2-rich. Not only did no bubbles nucleate, but expansion of the liquid, causing partial decrepitation of the inclusions, indicated that they were H_2O-rich. All samples except one (Sample no. 208014) were subjected to heating/freezing studies.

FLUID INCLUSION PETROGRAPHY

Pre-intrusion, metamorphic veins

Fluid inclusions in pre-intrusion, metamorphic quartz are dominantly vapor-rich and occur along secondary planes and grain-boundaries. Daughter minerals were rarely observed and in all cases appeared to be a mica mineral.

Table 4. --Summary of fluid inclusion petrography

RASS Sample no. (Drill hole no. - depth)	Stage	Dominant inclusion type	Approx. % that evolved CO_2 when crushed	3-phase CO_2 - H_2O?	Daughter minerals?
152515	3/4	L-rich[1]	40	Yes (<1%)	No
208004 (1-23.7)	Metamorphic	V-rich[2] (85%)	<1	Yes (<1%)	No
208014 (1-36.8)	3/4	L-rich	10	No	No
208044 (1-67)	Metamorphic	V-rich (>90%)	<1	Yes (<1%)	No
208060 (1-86.7)	4	L-rich (>99%)	85	No	Yes
208092 (1-172.5)	3	L-rich (>90%)	25	No	No
208209 (3-76.1)	1/2	V-rich	5	Yes	No
208346	Baid al Jimalah East	L-rich (>90%)	75	No	No
208411 (2-74.6)	4	L-rich (>99%)	5	No	No
208420 (3-102.2)	2	V-rich	5	Yes	No
208437 (4-94)	3	L-rich	0	No	No

[1] Liquid-rich fluid inclusions
[2] Vapor-rich fluid inclusions

Table 5.--Fluid inclusion heating data, freezing data, and salinities

RASS Sample no. (Drill hole no. and depth)	Stage	Temperature(° C) filling or decrepitation (no. of measurements) [mean]	Temperature(° C) CO_2 triple point (no. of measurements	Ice-melting temperature (° C) (no. of measurements)	Clathrate-melting temperature (°C)	Salinity in weight percent NaCl equivalent (no. of measurements) [Preferred salinity]
208004 (1-23.7)	Metamorphic	340-379 V[1] (6) 343-345 C[2] (3) 329-346 D[3] (3) [347]	-56.9 - -57.7 (8)	--	8.9-11.9 (10)	1.0-2.5 (4)
208014 (1-36.8)	3/4	163-353 L[4] (22) 388 V (1) 372 D (1) [330][5]	--	-0.3 - -7.3 (14)	7.1-13.5 (12)	0.5-10.9 (15) [4.5-10.9]
208044 (1-67)	Metamorphic	355-408 V (5) 340-385 C (6) 395 D (1) [371]	-57.1 - -57.2 (3)	--	7.3-12.0 (11)	3.5-6.5 (3) [<6.5]
208060 (1-86.7)	4	262-385 L (42) [337]	--	-0.9 - -5.4 (25)	0.2-10.1 (12)	1.6-8.4 (25) [4.8-7.4]
208092 (1-172.5)	3	306-352 L (6) 450 V (1) [330][6]	-56.9 (1)	-4.0 - -4.9 (3)	7.5-9.9 (6)	5.4-7.7 (4) [5.4]
208209 (3-76.1)	1/2	274-408 L (8) 336-394 V (8) 348-352 C (3) 443 D (1) [349]	-56.7 - -59.1 (8)	-3.4 - -4.2 (2)	7.6-10.9 (12)	1.4-6.7 (6) [1.4-5.0]
208346	Baid al Jimalah East	224-313 L (31) [268]	--	0.0 - -2.5 (33)	8.6-9.9 (2)	0-4.2 (33) [0-4.2]
208437 (4-94)	3	310-347 L (5) [330]	--	-4.3 (1)	9.0-9.4 (2)	6.9 (1) [<6.9]

[1] Fluid inclusion homogenized to vapor
[2] Fluid homogenized by critical phenomena
[3] Fluid inclusion decrepitated before homogenizing
[4] Fluid inclusion homogenized to liquid
[5] Data from late, low temperature, secondary inclusions were not included in the calculation of the mean temperature
[6] Temperature from single fluid inclusion that filled to vapor is excluded.

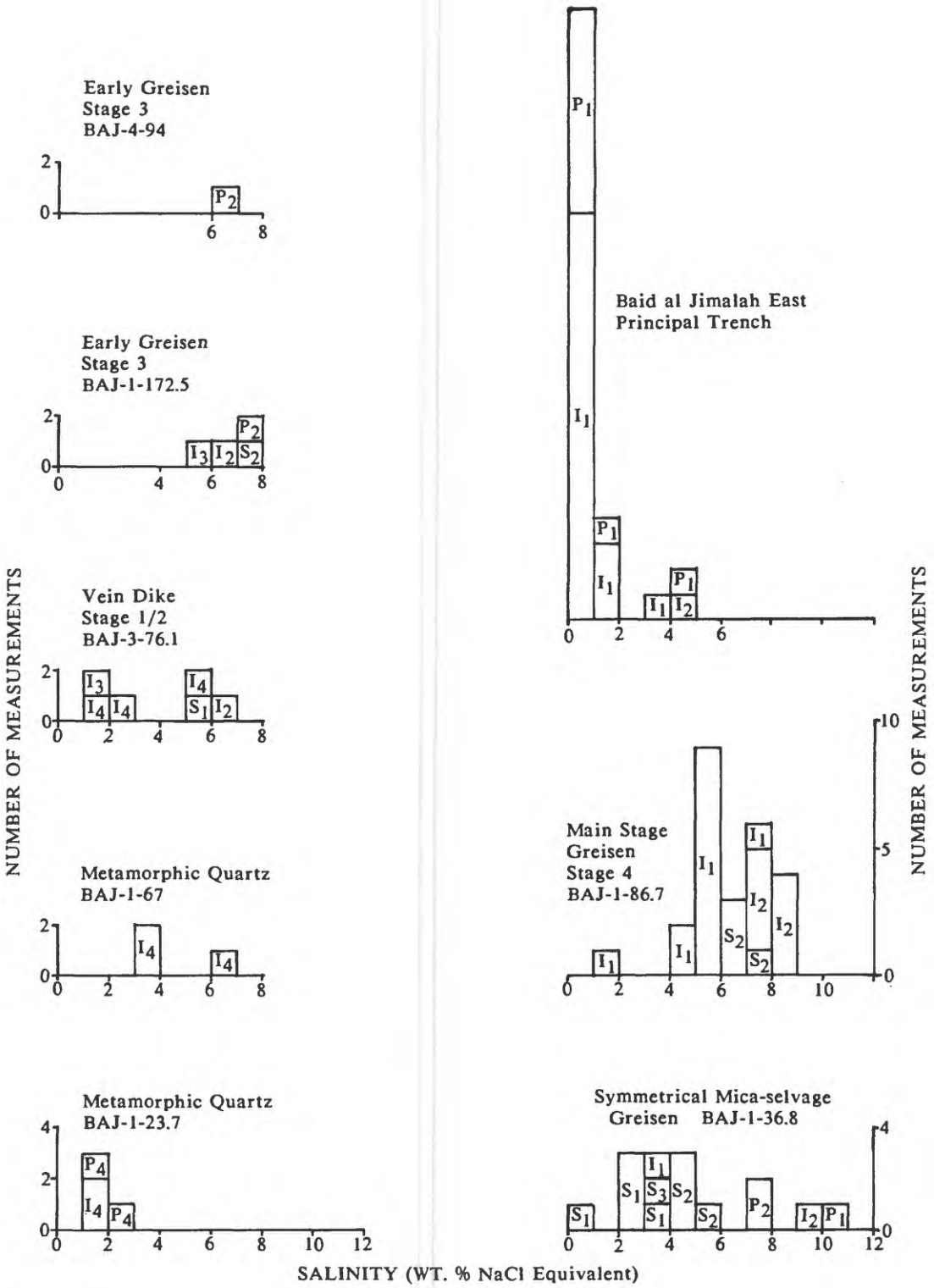

Figure 30.--*Histograms of fluid inclusion salinities for each sample studied. Primary and secondary fluid inclusions, and those of indeterminate origin are denoted by "P", "S", and "I", respectively. The subscripts, "1", "2", "3", and "4" denote: reliable salinities from ice-melting, "suspect" salinities from ice-melting, reliable salinities from clathrate-melting, and "suspect" salinities from clathrate-melting, respectively; e.g. "S_3" denotes a secondary fluid inclusion with a reliable salinity derived from clathrate melting.*

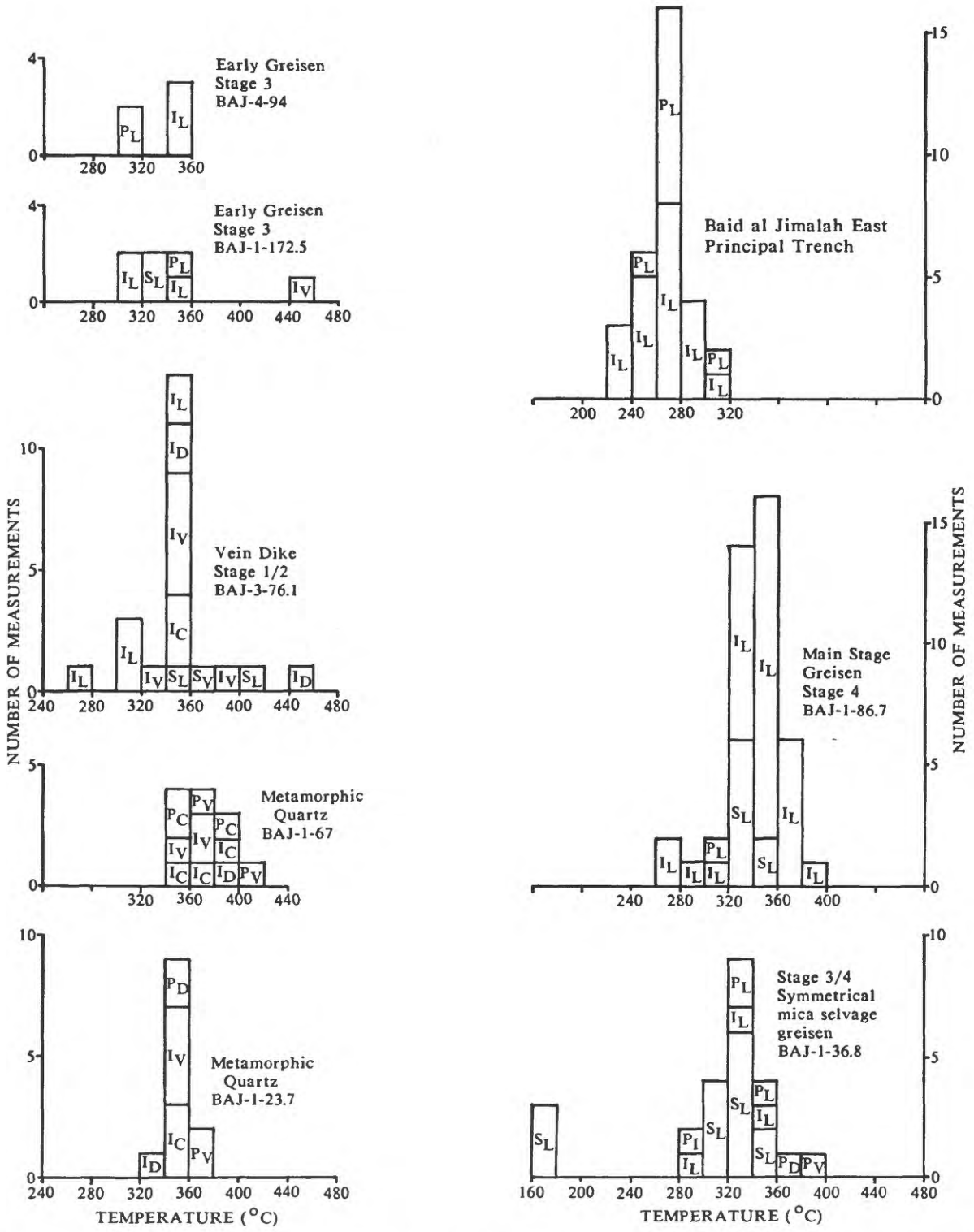

Figure 31.--*Histograms of fluid inclusion filling and decrepitation temperatures. Primary and secondary fluid inclusions, and those of, indeterminate origin are denoted by "P", "S", and "I", respectively, Filling to liquid, vapor, by critical phenomena, and decrepitation before filling are denoted by the subscripts "L", "V", "C", and "D", respectively; e.g. "P_L" denotes a primary fluid inclusion that filled to liquid.*

These daughter minerals may actually be accidental inclusions that caused imperfect growth of the quartz, thus forming the inclusion. If so, such inclusions would be primary. A few primary and possibly primary, three phase CO_2-H_2O inclusions were observed. The vast majority of inclusions are less than 10 microns in diameter.

The most striking feature of these inclusions is that they show partial decrepitation by natural means (also known as auto-decrepitation). Such inclusions are characterized by a halo of tiny secondaries around the larger, partially decrepitated, inclusion, and are commonly found in high grade, metamorphic rocks (Roedder, 1984). Because the Murdama graywacke has been subjected to only greenschist facies metamorphism, it is probable that the overheating that caused the partial decrepitation occurred during the intrusion of the Baid al Jimalah porphyry. No evidence of autodecrepitation was seen in any later stage.

Stages 1 and 2

Fluid inclusions in Stage 1 and Stage 2 quartz are essentially identical. Samples are characterized by the presence of both liquid- and vapor-rich primary inclusions. This fact is important to the interpretation of the evolution of the Baid al Jimalah hydrothermal system as well as the depth of mineralization, and will be discussed at length in a later section. A few, possibly primary, three-phase, CO_2-H_2O inclusions were observed. No daughter minerals were seen. Most inclusions are less than 10 microns, but a few are as large as 15 microns. Most of the inclusions in the samples occur along secondary planes and many inclusions are necked down, causing highly variable phase-ratios. Necked down inclusions were carefully avoided in the heating/freezing work.

Stage 3

The fluid inclusions of Stage 3 are dominantly liquid-rich, but there are some definite primaries that are vapor-rich. No daughter minerals were seen. Three phase, CO_2-H_2O inclusions are very rare. Evidence of necking down is common.

Stages 4 & 5

Fluid inclusions in Stages 4 and 5 are significantly different from those of the earlier stages. No vapor-rich inclusions were observed (except for ones which have formed by necking down). This is the only stage in which daughter minerals were observed. Inclusions contain a maximum of two daughter minerals. The most common is a birefringent, euhedral rod; The other is equant, anhedral, and apparently isotropic. Daughter minerals are not common and could not be identified as to mineral species. They showed no change upon heating or cooling. Despite the fact that most Stage 4 and 5 fluid inclusions are less than 10 microns in diameter, some are as large as 50 microns, making these very easy to work with. These large inclusions owe their origin to the vuggy nature of Stage 4 mineralization. No three-phase, CO_2-H_2O inclusions were observed.

CRUSHING STUDIES

Introduction

Crushing transparent minerals containing fluid inclusions in a special device that allows observation of the process under a microscope is a sensitive qualitative test for the gas composition of fluid inclusions. Nearly pure H_2O will not yield bubbles when a fluid inclusion is crushed in oil, because the internal pressure of the fluid inclusions is less than one atmosphere at room temperature. Fluid inclusions which contain CO_2 or other gases will evolve bubbles because the internal pressure is greater than one atmosphere at room temperature. CO_2 can be distinguished from CH_4 because bubbles of the latter will dissolve and disappear if the fluid inclusions are crushed in kerosine.

Pre-intrusion, metamorphic veins

Both samples that were crushed evolved very little CO_2, demonstrating that the majority of the secondary, vapor-rich fluid inclusions in the samples are dominated by H_2O. The origin of the secondary, vapor-rich inclusions is uncertain; the most likely explanation is that they were formed during the early hydrothermal history of the Baid al Jimalah deposit (Stage 1 and Stage 2), when the system contained a vapor phase.

Stages 1 and 2

The two Stage 1 and 2 samples that were crushed showed a small, but significant population of CO_2-bearing fluid inclusions (about 5 percent).

Stages 3, 4 and 5

Samples from Stages 3 and 4 stand in marked contrast to the the previous stages, because a large proportion of fluid inclusions (25-85%) streamed out CO_2 upon crushing. This was an entirely unexpected result because of the rarity of three phase, CO_2-H_2O inclusions observed in the sections. Nevertheless, the presence of abundant CO_2 was confirmed by the formation of clathrate compounds during the freezing studies (see below).

Baid al Jimalah East

The single quartz sample from Baid al Jimalah East that was studied is similar to those of Stages 3 and 4 in that no three phase, CO_2-H_2O fluid inclusions were observed, but about 75 percent of the inclusions streamed out CO_2 upon crushing. This adds support to the argument that the veins at Baid al Jimalah East were part of the Baid al Jimalah West hydrothermal system.

FREEZING STUDIES

Freezing data and inferred salinities are summarized in table 5 and fig. 30. The precision of the freezing data is within $\pm 0.1^{\circ}$ C, but the accuracies of the inferred salinities vary considerably among samples and among inclusions in the same sample. For this reason, salinity data have been differentiated as to reliability in fig. 30 and a preferred salinity range for each sample is indicated in brackets in table 5. Salinities are given as "weight percent NaCl equivalent" (wt

percent NaCl equiv.). This arises out of the assumption that the dominant ionic species in most H_2O-rich hydrothermal fluids is NaCl and that the salinities of hydrothermal fluids determined from freezing point depression of inclusion fluids and phase equilibria in the system NaCl-H_2O are a good approximation of fluid composition. Similarly, salinities derived from clathrate melting in CO_2-rich fluid inclusions and phase equilibria in the system H_2O-CO_2-NaCl are assumed to be a good approximation of composition in such fluids. Such is not always the case, as was found at Baid al Jimalah.

Salinity determinations were indeed complicated by the presence of CO_2 and CH_4. In addition to the crushing studies, the existence of CO_2 was confirmed by the presence of: (1) three-phase fluid inclusions with an observed triple point near -56.6° C, (the triple point of CO_2); (2) three separate freezing events upon cooling, and (3) the formation of a clathrate compound (that is, a gas hydrate). Salinities (as NaCl equivalent weight percent NaCl) can be accurately determined from freezing studies only if H_2O and ionic species in fluid inclusions are present, using data from the system H_2O-NaCl (Potter and others, 1978) or if three phase H_2O-CO_2 inclusions are present (Collins, 1979). The presence of CH_4 was confirmed by clathrate melting temperatures greater than 10° C and measured triple points for three phase inclusions as low as -59.1° C. No triple points at -56.6° C were measured, indicating that all inclusions had some other dissolved gas in addition to CO_2. Large amounts of most other common gases found in hydrothermal systems can be excluded because all three phase CO_2-H_2O inclusions showed homogenization of the two CO_2-rich phases at temperatures less than 31.1° C (the triple point of CO_2). SO_2, H_2S, and COS all have critical temperatures greater than 100° C, making it likely that any significant amount of these gases would raise the CO_2 homogenization temperature above the triple point. CH_4 is the only common gaseous species that can lower the triple point of the CO_2-rich phases as well as raise the clathrate melting temperature beyond 10° C (Burruss, 1981).

The presence of CO_2, CH_4 as well as C_2H_6 (ethane) and C_3H_8 (propane) was confirmed by decrepitating individual inclusions with a laser microprobe coupled with a mass spectrometer (M. Sommer, written commun.,1985), see table 6.

The salinity data in figure 30 are grouped in four categories. Data marked with the subscript, "1", were determined from freezing point depressions of ice in fluid inclusions which exhibited no evidence of CO_2 or CH_4 and are considered to be good data. Data marked with the subscript, "2", are from inclusions with detectable amounts of these gases. Inasmuch as the formation of a clathrate may increase the apparent salinity to twice that of the actual salinity, these data only serve to set an upper limit. Data marked with the subscript, "3", are those measured from the freezing point depression of clathrate in three phase CO_2-H_2O inclusions in which the triple point of the CO_2-rich phase was between -56.6° and -57.0° C. These are considered to be good data. Data marked with the subscript, "4", are from fluid inclusions with observed triple points less than -57.0° C, or with neighboring fluid inclusions with clathrate melting temperatures greater than 10° C (that is, those containing appreciable CH_4). The presence of CH_4 acts in opposition to the effect of NaCl and other ionic species (Collins, 1979), making these minimum salinites.

Table 6.--Quantitative fluid inclusion gas analyses.
Analyzed by M. Sommer, Geodynamics Inc. Houston, Texas

RASS Sample no. (Drill hole no. and depth)	Stage	CH_4/H_2O Molar ratios for individual fluid inclusions	CO_2/H_2O Molar ratios for individual fluid inclusions	Other species detected	Comments
208004 (1-23.7)	Metamorphic	0.0012 0.0011 0.0010 0.0012	0.0180 0.0170 0.0173 0.0195	Trace ethane (C_2H_6) Trace propane(C_3H_8)	No sulfur species detected
208014 (1-36.8)	3/4	0.0005 0.0005 0.0004 0.0005	0.0234 0.0249 0.0250 0.0236	Much propane	C_3H_8/H_2O molar ratio not quantifiable, but there is more C_3H_8 than CH_4.
208209 (3-76.1)	1/2	0.0013 0.0015 0.0011 0.0013	0.0935 0.0922 0.0904 0.0916	Trace propane Traces of other, unidentified hydrocarbons	No sulfur species detected.

Despite these uncertainties, it is possible to make some generalizations about the salinites of the hydrothermal fluids at Baid al Jimalah.

1. All salinities are less than 11 wt percent NaCl equiv.

2. Salinities for metamorphic quartz are between 1.0 and 6.5 wt percent NaCl equiv.

3. Salinites in Stages 1 and 2 are lower, with a preferred range of 1.4-5.0 wt percent NaCl equiv. Although both liquid- and vapor-rich populations of fluid inclusions exist, no difference was seen between the salinities of the two populations. Normally, the liquid-rich inclusions would be more saline than the vapor-rich inclusions.

4. The main stage hydrothermal fluids (Stages 3, 4 and 5) are more saline than those of Stages 1 and 2, with a preferred range from 4.5 to 10.9 wt percent NaCl equiv. (Salinities less than 4.0 equiv. wt percent NaCl in Sample no. 208014 (Stages 3 and 4) are due to the presence of late, low temperature (T_h<180° C), secondary fluid inclusions.)

5. Salinities at Baid al Jimalah East range from 0 to 4.2 wt percent NaCl equiv., with the great majority less than 1 wt percent NaCl equiv.

FILLING TEMPERATURES

Filling temperatures and the manner of filling are summarized in table 5 and figure 31. As with the freezing data the precision of the heating data is $\pm 0.1^{\circ}$ C. The accuracy varies according to the phenomenon being observed. Data on fluid inclusions filling to liquid (that is, bubble disappearance) are better than $\pm 1^{\circ}$ C; filling near the critical point are better than $\pm 5^{\circ}$ C; filling to vapor are better than $\pm 10^{\circ}$ C. Data on decrepitation before filling is better than $\pm 1^{\circ}$ C. Filling to liquid, vapor, critical point, and decrepitation before filling are signified by the subscripts "L", "V", "C", and "D", respectively, in figure 31. None of the filling temperatures have been corrected for pressure to reflect the actual trapping temperatures.

Pre-intrusion, metamorphic quartz

Filling and decrepitation temperatures for the pre-intrusion metamorphic veins range from 329° C to 408° C, with a mean of 347° C for sample no. 208004 and 371° C for sample no. 208044. These mean temperatures are close to the minimum for the lower greenschist facies, ca. 380° C (Winkler, 1967), and are reasonable for the metamorphic grade of the Murdama rocks, although actual temperatures of trapping may be higher. All of the measured fluid inclusions in the pre-intrusion, metamorphic quartz samples filled to vapor or exhibited critical phenomena. As the compressibility of fluids near the critical point or in the vapor field is large relative to fluids in the liquid field (that is, isochores on a pressure-temperature diagram have a shallow slope), it is possible that the pressure correction for temperature could be large.

Stages 1 and 2

Filling and decrepitation temperatures show a wide range, from 274° C to 408° C, but with a large population between 340° C and 360° C, yielding a mean temperature of 349° C. A significant difference between the metamorphic quartz and Stages 1 and 2 is that some primary fluid inclusions filled to liquid and others filled to vapor. This strongly implies that the hydrothermal fluids during this stage were in the two phase field due to the large miscibility gap in the system H_2O-CO_20-NaCl.

Stages 3, 4, and 5

Almost all of the fluid inclusions measured in quartz from Stages 3, 4, and 5 filled to liquid, indicating that the fluids which precipitated the main stage greisen mineralization were in the liquid field. Of 77 measurements, two inclusions filled to vapor and one decrepitated. As is the case with the salinities, there is no detectable difference in the filling temperatures among the three stages; temperatures range from 262° C to 450° C. Despite this broad range, there is actually a tight grouping of data between 320° C and 360° C (fig. 31), with mean values for the four samples analyzed clustered between 330° C and 337° C.

Stage 6

Although no Stage 6 specimens observed had usable fluid inclusions, it is clear from fluid inclusion petrography and a few analyses of secondary fluid inclusions in sample no. 208014, that there was a significant hydrothermal history with temperatures as low as 160° C, postdating the main stage greisen mineralization.

Baid al Jimalah East

All fluid inclusions from Baid al Jimalah East filled to liquid in the temperature range, 224° to 313° C, with a large peak between 260° and 280° C.

DEPTH OF MINERALIZATION AND PRESSURE CORRECTIONS FOR FILLING TEMPERATURES

The fact that high salinity fluid inclusions were not observed allows us to place an absolute minimum on the depth of mineralization at Baid al Jimalah. Because Stage 2 vein-dikes contain aplite, they must have formed at temperatures at or above the granite solidus. Even at a pressure (P_{H2O}) of 1000 kg/cm^2 (about 1 kb) and 2.5 wt percent fluorine (both figures are higher than those for Baid al Jimalah granite) the granite solidus is 580° C (Anfilogov and others, 1973). Using a salinity for Period 1 fluids of 5 wt percent NaCl (table 5), a temperature of 580° C, and the data of Sourirajan and Kennedy (1962), we derive a minimum pressure of 800 bars. Any less pressure would drop the hydrothermal fluid into a two-phase field, one phase being vapor-rich and low salinity, the other being liquid-rich and high salinity. This corresponds to a minimum depth of about 3.1 km, assuming a lithostatic load and a rock density of 2.67g/cm^2. (The reason we observe low salinity liquid- and vapor-rich fluid inclusions in Period 1 veins is due to immiscibility in the system H_2O-CO_2.) A maximum depth can also be derived using the same temperature and salinity, plus the data of Potter (1977).

In order to account for the 231° C difference between the mean filling temperature of 349° C for Period 1 fluid inclusions (table 5) and the 580° C solidus mentioned above, we infer a pressure of 2.2 kilobars and a depth of 8.4 km. This rather high calculated pressure and great depth does not seem reasonable, given the porphyritic nature of the Baid al Jimalah granite. The preponderance of fluid inclusions filling to vapor or showing critical phenomena implies that the appropriate isochores have shallow slopes, making it possible for a relatively small difference between the pressure at trapping and the pressure at filling to account for the large difference between the trapping temperature and the filling temperature. This effect is enhanced by the presence of CO_2 and CH_4, which sharply decreases the critical point temperature (Burruss, 1981, figs. 3.4 and 3.11). Thus, the use of Potter's pressure correction data for calculating the maximum depth is inappropriate. Nevertheless, a relatively deep environment is consistent with the observed plastic deformation and boudinage of the metamorphic and Period 1 veins.

We can apply the minimum pressure of 800 bars to correct the filling temperatures of those fluid inclusions which exhibited no evidence of containing appreciable CO_2, namely some of the data from Stages 3, 4, and 5, and from Baid al Jimalah East. Using the data of Potter (1977) - which is safer here because of the lack of observed critical phenomena - we find that the probable trapping temperatures of the main stage greisen mineralization at Baid al Jimalah West are about 80° C higher than the filling temperatures, that is, 410-417° C. The pressure correction for Baid al Jimalah East is about 75° C, making the probable trapping temperatures about 343° C rather than 268° C. It must be emphasized that these corrections are only rough estimates because of the lack of PVT data in the system which is really pertinent, H_2O-NaCl-CO_2-CH_4.

ORE GENESIS MODEL

Deposits of tungsten, tin, and molybdenum associated with specialized granites offer some of the most compelling evidence extant that ore-forming fluids exsolve directly from magma. Such is the case with Baid al Jimalah. In addition to the evidence from the rock geochemistry and spatial association of the deposit with the intrusion, several features of the granite and veins confirm this interpretation.

The presence of a truly aplitic groundmass near the margins of the main cupola (fig. 8), giving way downward to less aplite and increasing amounts of seriate groundmass similar to the earlier, higher level dikes and sill-like bodies, as well as the highly variable groundmass size and phenocryst content, is strong evidence for the concentration of volatile components near the apex of the cupola, exsolution of an H_2O-rich, CO_2-bearing fluid, and rapid pressure-quenching of the magma. Similar variable textures were observed to a lesser extent in the lower sill-like body in DDH-BAJ-6 (47-68.5 m), indicating that this intrusive body was also a source of hydrothermal fluids. Such variability in texture is highly characteristic of igneous cupolas that have exsolved hydrothermal fluids (White, and others 1981) and suggests strongly that the granite porphyry found at depth in drill holes BAJ-1 and BAJ-6 is the source of the mineralization at Baid al Jimalah. The relatively uniform texture of most of the dikes and sill-like bodies at or near the surface suggests that these rocks were a minor source of hydrothermal fluids and acted mainly as a host to the veins.

The vein-dikes of Stage 2 offer the strongest evidence for the magmatic origin of at least the early quartz-molybdenite mineralization. These structures, with characteristics of both igneous dikes and hydrothermal veins, record the transition from predominately igneous to predominantly hydrothermal processes (White and others, 1981). Upon exsolution of an aqueous-rich phase (or phases) from the magma, the internal pressure of the intrusion rose almost instantaneously, due to the volume increase of the system, causing hydrofracturing of the country rock. The actual occurrence of pressures greater than lithostatic were documented by Kamilli (1978) at the Henderson molybdenum deposit in Colorado. These fluids then moved out from the magma through the stockwork fractures, relieving the over-pressure and precipitating quartz and molybdenite as it went. In some cases, the fractures were then invaded by the remaining igneous melt. Because of its greater viscosity, the melt could travel only a short distance from the country rock-magma contact. The plastic deformation and boudinage apparent in Stage 1 and 2 veins indicate that the Murdama graywacke was at a high temperature (probably 600^{o}-700^{o} C) and that the magma was still intruding and deforming the country rock even though most of it had crystallized and had evolved an aqueous phase.

It is apparent from the fluid inclusion studies, however, that there probably was some contribution of components from the Murdama country rocks. That the pre-intrusion metamorphic rocks contained considerable CH_4 is evident from the fluid inclusion data from the metamorphic veins, which show clathrate melting temperatures greater than 10^{o} C. CH_4, which is present in most of the other samples analyzed in the fluid inclusion study, could have entered the igneous-hydrothermal system either by assimilation of Murdama rocks or by scavenging by circulating groundwater later in the history of the hydrothermal system. The dominant means was probably the latter, because CH_4 is generally a very minor component in magmas (White and Waring, 1963). Some CH_4 must have been in the magma, however, because we see evidence of it in Stage 1 and 2 veins, the constituents of which we know came directly from the intrusion.

The following is a proposed model for the genesis of the Baid al Jimalah tungsten deposit, based largely on the data presented in this report, but also drawing on data and interpretations of Elliott and Cole (1986) and Lofts (1982).

1. The highly differentiated Baid al Jimalah granite intruded along a northwest-trending fault that roughly coincides with a broad anticlinal warp in the unconformable base of the Jurdhawiyah group (Lofts, 1982). Intrusion of dikes and sill-like bodies preceeded the main cupola, which was emplaced by a combination of stoping and upwarping of the Murdama. Although it is difficult to demonstrate upwarping of the Murdama as a means of accommodating the magma because of the general lack of observable bedding, the plastic deformation and boudinage seen in Stage 1 and 2 veins suggest that this was a mechanism of intrusion. Depth of emplacement of the magma was greater than 3.1 km, assuming a lithostatic load and a pressure of greater than 800 bars.

2. Contact metamorphism of the Murdama graywacke and diabase formed quartz-biotite-cordierite hornfels and feldspathic quartz-biotite hornfels, respectively.

3. The magma crystallized and exsolved a hydrothermal fluid at or near magmatic temperatures (580°-700° C for a fluorine-rich melt). The aqueous fluid was rich in CO_2, contained some methane and higher order hydrocarbons, and had a salinity of 1.4 - 5 wt percent NaCl equiv. Pressure and temperature conditions were such that the fluid instantly separated into two immiscible phases, one low density and CO_2-rich, the other high density and H_2O-rich. The exsolution of the hydrothermal fluid raised the hydrostatic pressure in the intrusion to greater than lithostatic, to the point where the Murdama hornfels underwent hydrofracturing, forming a stockwork, Stage-1 quartz-molybdenite veins, and Stage-2 vein-dikes.

4. A hydrothermal system, at least 7 km^2 in areal extent, formed. This estimate is based on the size of the fluorine anomaly (Lofts, 1982). If we include the veins at Baid al Jimalah East, the system becomes as large as 12.5 km^2.

5. Stage-3, feldspar-stable veins formed at temperatures between 410° C and 420° C. Hydrothermal fluids were in the liquid field and had salinities of 4.8-10.9 wt percent NaCl equiv. Mineralization at Baid al Jimalah East probably commenced at about this time and continued for the rest of the life of the Baid al Jimalah hydrothermal system. Temperatures and fluid salinities at Baid al Jimalah East were 299°-388° C and 0-4.2 wt percent NaCl equiv., respectively.

6. Minor strike-slip movement along the northwest-trending fault that transects the Baid al Jimalah West deposit caused the shear stresses that formed the dominant vein-trend of N60°-75°W.

7. Main stage (Stages 4 and 5) mineralization caused greisenization of wall rock and earlier veins at temperatures similar to those of Stage-3 and deposited most of the wolframite. Greisen alteration is best thought of as a special type of quartz-sericite-pyrite (that is, phyllic) alteration, formed by the breakdown of feldspar to form muscovite and quartz, plus the addition of silica and other components by the hydrothermal fluids. The basic reaction is the well-known hydrolysis reaction of Hemley and Jones (1964) in which muscovite and quartz are formed at the expense of potassium feldspar:

$$3\ KAlSi_3O_8 + \underbrace{2\ H^+}_{\text{fluid}} = KAl_3Si_3O_{10}(OH)_2 + 6\ SiO_2 + \underbrace{2\ K^+}_{\text{fluid}}$$

A similar equation can be written for the albite component of the feldspars, which also involves K-Na exchange:

$$3\ NaAlSi_3O_8 + \underbrace{K^+ + 2\ H^+}_{\text{fluid}} = KAl_3Si_3(OH)_2 + 6\ SiO_2 + \underbrace{3\ Na^+}_{\text{fluid}}$$

The release of the small amount of Ca^{2+} from the plagioclase during greisenization was probably an important source of Ca^{2+} for the formation of fluorite and the replacement of wolframite by scheelite in Stage 5 in such a low Ca^{2+} system:

$$3\ CaAl_2Si_2O_8 + \underbrace{4\ HF + 2\ K^+}_{\text{fluid}} = 2\ KAl_3Si_3O_{10}(OH)_2 + 2CaF_2 + \underbrace{Ca^{2+}}_{\text{fluid}}$$

The release of Fe^{2+} and Mn^{2+} from previously deposited wolframite (and Fe^{2+} from greisenization of biotite) could then provide much of these two elements for the formation of the late manganosiderite:

$$1/2\ FeMn(WO_4) + \underbrace{Ca^{2+} + H_2O + CO_2}_{\text{fluid}} = CaWO_4 + 1/2\ FeMn(CO_3)_2 + \underbrace{2\ H^+}_{\text{fluid}}$$

Replacement of wolframite by scheelite has also been reported by Karwowski (1975). Based on the phase equilibria presented by Burt (1981), the paucity of topaz at Baid al Jimalah, in addition to the the presence of scheelite, both imply that fluorine fugacity was low compared to other greisen deposits. This observation is supported by the relatively low fluorine content of fresh Baid al Jimalah granite (0.26 weight percent in Sample no. 889494 compared to the 0.37 weight percent average for specialized granites - table 1).

8. Late, Stage-6 mineralization was dominated by drusy and chalcedonic quartz and calcite at temperatures at least as low as 235° C, in large part localized along the WNW-trending shear zone. Hydrothermal fluid salinites were 0.5-3.0 wt percent NaCl equiv.

COMPARISON WITH SIMILAR DEPOSITS

Of the greisen deposits known to the author, the ones most similar to Baid al Jimalah exist in southwest England. These include Cligga Head (Jackson and others, 1977), Bostraze-Balleswidden (Jackson and others, 1982), St Michael's Mount (Jackson and Rankin, 1976), and especially Goonbarrow (Bray and Spooner, 1983; Alderton and Rankin, 1983; Rankin and Alderton, 1983) and Hemerdon (Rankin and Alderton, 1983; Christofferson, 1982; Skillings, 1980). Baid al Jimalah also exhibits intriguing and instructive similarities to Climax-type molybdenum deposits.

The deposits cited for southwest England are all characterized by a close spatial, temporal, and genetic association with porphyritic, specialized granites and by dominantly parallel or sub-parallel sheeted veins with greisen alteration envelopes and varying amounts of tungsten and tin. Grades at Baid al Jimalah are very similar to those at Hemerdon. The mean WO_3 and Sn grades for Hemerdon are 0.115 and 0.023 weight percent, respectively (Christofferson, 1982); the arithmetic mean grades for Baid al Jimalah are 0.117 and 0.012, respectively (Lofts, 1982). The total tonnage (not necessarily economic) for Hemerdon is 174.5 million metric tons; the total for Baid al Jimalah (calculated to only a 25 meter depth) is 10 million metric tons. The tonnage figure for Baid al Jimalah is misleadingly low, however, because the two drill holes that bottomed in the granite cupola (BAJ-1 and BAJ-6 at depths of 139 and 180 meters, respectively) had average grades for WO_3 of 0.119 and 0.121 weight percent, respectively, and average grades for Sn of 0.004 and 0.005 weight percent, respectively. Thus ore grade mineralization exists at depths greater than 25 m, but a deep open pit or an underground mine would be required to extract it.

Major differences between Baid al Jimalah and other deposits are the lack of kaolinization that is so characteristic of such deposits as Cligga Head, Bostraze-Balleswidden, Goonbarrow, and Hemerdon and the relative lack of

tourmaline and topaz at Baid al Jimalah. The deposits in southwest England formed at depths of about 1-2 km. (Jackson and others, 1977) whereas Baid al Jimalah probably formed at a depth of greater than 3.1 km.

Higher fluid inclusion homogenization temperatures (400° - >500° C) than those observed at Baid al Jimalah are reported for Bostraze-Balliswidden (Jackson and others, 1982) and the St. Austell granite (including Goonbarrow) (Alderton and Rankin, 1983), but when the filling temperatures at Baid al Jimalah are corrected for pressure, the temperatures are much closer. Homogenization temperatures for greisen mineralization at Baid al Jimalah are in the same range as those reported by Roedder (1984, table 15-7) for tin-tungsten greisens throughout the world. Maximum salinity (10.9 wt percent NaCl equiv.) at Baid al Jimalah is lower than most greisen deposits, which commonly have salinities as high as 65 weight percent NaCl (Roedder, 1984, table 15-7). This is probably due to the greater depth of mineralization, causing the hydrothermal fluid to be above the two phase field in the system H_2O-NaCl. Daughter minerals are correspondingly rare.

Unlike Baid al Jimalah, liquid CO_2 is uncommon in the English deposits, with the exception of Hemerdon and Goonbarrow (Rankin and Alderton, 1983), but is widely reported from other Sn-W deposits (Roedder, 1984), including Jabal al Gaharra in Saudi Arabia (Elliott, 1980). This author has found no other reference to any tungsten deposit with the abundance of CH_4 seen at Baid al Jimalah.

The age difference between Baid al Jimalah (569 Ma) and the English deposits (260-280 Ma) is not surprising in the context of their tectonic setting. Baid al Jimalah (and Jabal al Silsilah) formed near the end of the Proterozoic Pan-African orogeny and the English deposits formed near the end of the Hercynian orogeny. Plutonism in both areas is intracratonic and is the product of continental collision (Stoeser and Camp, 1984; Perroud and others, 1984; Sawkins, 1984)

Baid al Jimalah also has a number of similarities to Climax-type molybdenum deposits. Besides the obvious association with specialized granites, the Baid al Jimalah West deposit and the Climax and Henderson deposits all have early quartz-molybdenite stockwork veins. Both Climax and Henderson have steeply-dipping, late veins and fractures with quartz-sericite-pyrite envelopes that cut the molybdenite mineralization, and contain most, if not all of the wolframite and topaz that occur at these two deposits. These veins are therefore directly analogous to the main-stage greisen veins at Baid al Jimalah. The major difference among these deposits is therefore quantitative rather than qualitative. Climax-type deposits are dominated by early quartz-molybdenite stockwork veins, whereas Baid al Jimalah is dominated by late quartz-tungsten sheeted veins. The maximum value of WO_3 at Climax is 0.05 (R.P. Smith, oral commun., 1985) and 0.005 at Henderson (R. Carten, oral commun., 1985). This combination of early quartz-molybdenite plus later sheeted quartz-wolframite veins is seen in many of the major southeast China tungsten deposits (Gary Landis, oral commun., 1985). It is quite possible that a careful search at other deposits, such as Hemerdon, would also reveal early quartz-molybdenite veining. This general similarity between Climax-type deposits and Sn-W greisen deposits was first pointed out by Burt (1981), who refers to Climax-type deposits as "porphyry-greisens".

RECOMMENDATIONS FOR EXPLORATION

The paleosurface reconstruction by J. Cole (oral commun., 1985) indicates that relatively little of the Murdama has been eroded since the Precambrian. Thus, there is considerable likelihood that other mineralized cupolas are sufficiently near the surface to be feasible mining prospects. The most obvious prospecting tool would be the identification of zones of hornfels in the Murdama in areas with no exposed igneous rock. Geochemical exploration of both primary dispersion halos and heavy mineral concentrates in Wadi sediments, based on elements associated with greisen deposits, would be highly useful. Based on experience at Baid al Jimalah (Lofts, 1982) and Jabal as Silsilah (Du Bray and others, 1984), useful pathfinder elements, in decreasing order of areal dispersion would be As, Pb, F, Rb, W, Sn. Boron, which is frequently cited as a pathfinder element for greisen deposits (Levinson, 1980 p. 55), would probably not be of much use, given the lack of boron-bearing minerals at Baid al Jimalah and Jabal as Silsilah. Detailed gravity surveys on a 500 meter grid, given the generally small size of associated granite bodies, would be the most rewarding geophysical method.

CONCLUSIONS

The principal conclusions of this study are:

1. The Baid al Jimalah tungsten deposit is the result of a single cycle of igneous intrusion and hydrothermal mineralization. Although the deposit has not been drilled out, little potential exists for higher grades at depth than those already found.

2. The deposit is typical of sheeted vein tungsten deposits associated with highly differentiated granites found elsewhere in the world, especially in southwest England. It also has a strong genetic affinity to Climax-type molybdenum deposits found in western North America. Baid al Jimalah (and perhaps other similar tungsten deposits) has a weak, early stage of quartz-molybdenite stockwork veining and a relatively strong later stage of tungsten mineralization associated with greisen alteration. Climax-type deposits have several strong quartz-molybdenite stockwork-veining events, followed by (an equal number of?) greisenizing events with weak tungsten mineralization. The difference between the two deposit types is therefore one of relative importance of early molybdenite versus later wolframite mineralization. The chemistry of the associated granite porphyries and the mineral assemblages involved are virtually identical.

3. Early quartz-molybdenite mineralization formed in a stockwork at magmatic temperatures (ca. 580°-700 °C) from a fluid that was in the two phase field. One phase was low density and relatively rich in CO_2; the other phase was of a higher density and relatively rich in H_2O. The quartz-molybdenite mineralization probably precipitated from the latter phase.

4. Early main stage mineralization was characterized by the stability of feldspar. This gave way to the more typical greisen assemblage of quartz + muscovite. Wolframite became unstable during the latter stage of the greisen mineralization and was progressively replaced by scheelite.

5. Temperatures of the greisen mineralization were largely between 410° and 420° C; salinities were 4.5-10.9 NaCl equivalent weight percent.

6. Depth of mineralization was greater than 3.1 km.

7. CO_2 and CH_4 were important volatile components in addition to H_2O and HF. Higher order hydrocarbons were also present.

8. A reasonable possibility exists for the presence of similar, shallow, buried deposits - perhaps higher in grade - in the Afif terrane of the Saudi Arabian Shield.

DATA STORAGE

All data used in the preparation and writing of this report, as well as some data that was not used, are stored in Data File USGS-DF-06-8, the contents of which are listed below.

(1) Trench maps

(2) Author's manuscript

(3) Core logs

(4) Petrographic, analytical, and fluid inclusion data listed by RASS sample number.

MINERAL OCCURRENCE DOCUMENTATION SYSTEM (MODS)

Data on mineral occurrences recorded in this report have been entered or updated as follows:

MODS Number	Occurrence name	Comments
00960	Baid al Jimalah East	Existing MODS file updated September 1986
02661	Baid al Jimalah West	Existing MODS file updated September 1986

REFERENCES CITED

Alderton, D. H. M., and Rankin, A. H., 1983, The character and evolution of hydrothermal fluids associated with the kaolinized St. Austell granite, SW England: Journal Geological Society London, v. 140, part 2, p. 297-310.

Anfilogov, V. N., Glyuk, D. S., and Trufanova, L. G., 1973, Phase relations in interaction between granite and sodium fluoride at water vapor pressure of 1000 kg/cm^2: Geochemistry International, V.10, p. 30-33.

Boyle, D. Mck. and Howes, D. R., 1983, Assessment of the gold potential of the Nafud al Urayq area, northwest Najd: Saudi Arabian Deputy Ministry for Mineral Resources Open-File Report RF-OF-03-9, 58 p.

Bray, C. J., and Spooner, E. T. C., 1983, Sheeted vein Sn-W mineralization and greisenization associated with economic kaolinization, Goonbarrow china clay pit, St. Austell, Cornwall, England: Geologic relationships and geochronology: Economic Geology, v. 78, no. 6, p. 1064-1089.

Buma, G., Frey, F. A., and Wones, D. R., 1971, New England granites: trace element evidence regarding their origin and differentiation: Contributions to Mineralogy and Petrology, v. 31, p. 300-320.

Burruss, R. C., 1981, Analysis of phase equilibria in C-O-H-S fluid inclusions: in Short course in fluid inclusions: Applications to petrology, L.S. Hollister and M.L. Crawford, eds., Mineralogical Association of Canada, p. 39-74.

Burt, D. M., 1981, Acidity-salinity diagrams - application to greisen and porphyry deposits: Economic Geology v. 76, p. 832-843.

Christofferson, J. E., 1982, Town and country planning act, 1971; AMAX Exploration of U.K. Inc.; Hemerdon Mining and Smelting (U.K.) Ltd.; Hemerdon Mine; Public Inquiry; Proof of evidence of Jan Erik Christofferson B.Sc.: AMAX Exploration of U.K. Inc., Hemerdon Mine, Plympton, Plymouth, 19 p.

Cole, J. C., 1981, Reconnaissance geology of the Al Jurdhawiyah Quadrangle, Sheet 25/42 D, Kingdom of Saudi Arabia: Deputy Ministry of Mineral Resources, Kingdom of Saudi Arabia; Misc. Map 44, SA(IR)-374, marginal text, scale 1:100,000.

Cole, J. C., 1985a, Reconnaissance geology of the Al Abanat quadrangle, sheet 25/42 B, Kingdom of Saudi Arabia: Saudi Arabian Deputy Ministry for Mineral Resources Open-File Report USGS-OF-05-17, 66 p., scale 1:100,000. Also 1985, U.S. Geological Survey Open-File Report 85-721.

Cole, J. C., 1985b [1986], Geology of the Aban al Ahmar quadrangle, sheet 25 F, Kingdom of Saudi Arabia: Saudi Arabian Deputy Ministry for Mineral Resources Open-File Report USGS-OF-04-9, 86 p., scale 1:250,000. Also, in press, Saudi Arabian Deputy Ministry for Mineral Resources Geoscience Map GM-105-A.

Cole, J. C., Smith, C. W., and Fenton, M. D., 1981, Preliminary investigation of the Baid al Jimalah tungsten deposit, Kingdom of Saudi Arabia: Saudi Arabian Deputy Ministry for Mineral Resources Technical Record 20, 26p. Also, 1981, U.S. Geological Survey Open-File Report 81-1223.

Collins, P. L. F., 1979, Gas hydrates in CO_2-bearing fluid inclusions and the use of freezing data for estimation of salinity: Economic Geology, v. 74, p. 1435-1444.

Du Bray, E. A., 1984, Geology of the Silsilah ring complex, Kingdom of Saudi Arabia: Saudi Arabian Deputy Ministry of Mineral Resources; Technical Record USGS-TR-04-19 (IR 697), 78 p. Also, 1985, U.S. Geological Survey Open-File Report 85-253.

Du Bray, E. A., Smith, C. W., Samater, R. M., 1984, Result of grid sampling and large-scale geologic mapping, Silsilah tin deposit, Kingdom of Saudi Arabia: Saudi Arabian Deputy Ministry for Mineral Resources Open-File Report USGS-OF-04-47. Also, 1985, U.S. Geological Survey Open-File Report 85-10.

Elliott, J. E., 1985, Tin-bearing granite of Jabal al Gaharra in the southern Arabian Shield, Kingdom of Saudi Arabia: Saudi Arabian Deputy Ministry for Mineral Resources Professional Paper PP-2, p. 3-17.

Evensen, N. M., Hamilton, P. J., and O'Nions, R. K., 1978, Rare-earth abundances in chondritic meteorites: Geochimica et Cosmoschimica Acta, v. 42, p. 1199-1212.

Fakhry, A. O., 1941, Number 2 report, trip (in the northeastern Hijaz) from 1 March to 30 May 1941: Saudi Arabian Directorate General of Mineral Resources Open-File Report 20, 22 p.

Gordon, G. E., Randle, K., Goles, G., Corliss, J., Beeson, M. and Oxley, S., 1968, Instrumental activation analysis of standard rocks with high resolution gamma-ray detectors: Geochimica et Cosmochimica Acta, v. 32, p. 369-396.

Hemley, J. J. and Jones, W. R., 1964, Chemical aspects of hydrothermal alteration with emphasis on hydrogen metasomatism: Economic Geology, v. 59, p. 538-569.

Jackson, N. J., and Rankin, A.H., 1976, Fluid inclusions studies at St. Michael's Mount: Proceedings of the Ussher Society, v. 3, p. 430-434.

Jackson, N. J., Halliday, A.N., Sheppard, S.M.F., and Mitchell, J.G., 1982, Hydrothermal activity in the St. Just mining district, Cornwall, England: in Metallization Associated with Acid Magmatism, A.M. Evans, ed., John Wiley & Sons Ltd, p.137-179.

Jackson, N. J., Moore, J. McM. Moore, and Rankin, A.H., 1977, Fluid inclusions and mineralization at Cligga Head, Cornwall, England: Journal Geological Society of London, v. 134, p. 343-349.

Kamilli, R. J., 1978, The genesis of stockwork molybdenite deposits: implications from fluid inclusions from the Henderson Mine [abs.]: Geol. Soc. of America, Abstracts with Programs, v. 10, no. 7, p.431.

Karwowski, L., 1975, Tungsten mineralization in greisens of the Izera Upland (in Polish): Przeglad Geoloficzny, v. 23, p. 3-8.

Kleinkopf, M. D., and Cole, J. C., 1982, Geologic interpretation of geophysical data for the Wadi al Jarir and Al Jurdhawiyah quadrangles, sheets 25/42 C and D, Kingdom of Saudi Arabia: Saudi Arabian Deputy Ministry for Mineral Resources Open-File Report USGS-OF-03-1, 29p. Also, 1983, U.S. Geological Survey Open-File Report 83-371.

Krauskopf, K. B., 1967, Introduction to geochemistry: New York, McGraw-Hill, 721 p.

Levinson, A. A., 1980, Introduction to exploration geochemistry: Applied Publishing Ltd., Wilmette, Illinois, 2nd ed., 924 p.

Lofts, P. G., 1982, A preliminary evaluation of the Baid al Jimalah tungsten prospect: Saudi Arabian Deputy Ministry for Mineral Resources Open-File Report RF-OF-02-21, 223 p.

Moore, J. McM., 1979, Primary and secondary faulting in the Najd fault system, Kingdom of Saudi Arabia: U.S. Geological Survey Saudi Arabian Mission Project Report 262, 22p. Also, 1979, U.S. Geological Survey Open-File Report 79-1161.

Mytton, J. W., 1970, Reconnaissance for mineral deposits in the Precambrian rocks of the Wadi ar Rimah quadrangle, Kingdom of Saudi Arabia: U.S. Geological Survey Open-File Report (IR)SA-121, 75p.

Perroud, H., Van der Voo, R., and Bonhommet, N., 1984, Paleozoic evolution of the Armorica plate on the basis of paleomagnetic data: Geology, v. 12, no. 10, p. 579-582.

Potter, R. W., III, 1977, Pressure correction for fluid-inclusion homogenization temperatures based on the volumetric properties of the system NaCl-H_2O: Journal of Research U.S. Geological Survey, V. 5, no. 5, p. 603-607.

Potter, R. W., II, Clynne, M.A., and Brown, D.L., 1978, Freezing point depression of aqueous sodium chloride solutions: Economic Geology, v. 73, no. 2, p. 284-285.

Rankin, A. H., and Alderton, D.H.M., 1983, Fluid inclusion petrography of SW England granite and its potential in mineral exploration: Mineralium Deposita, v. 18, p. 335-347.

Riedel, W., 1929, Zur Mechanik geologisher Brucherscheinungen: Centralblat forschrift Mineralogie, Abt. B, 1929, p. 354-368.

Roedder, E., 1984, Fluid inclusions: Reviews in Mineralogy, Mineralogical Society of America, 644 p.

Sawkins, F. J., 1984, Metal deposits in relation to plate tectonics: Springer-Verlag, New York, 325 p.

Skillings, D. N., Jr., 1980, AMAX-Hemerdon venture evaluating major tungsten-tin property: Skillings Mining Review, v. 69, no. 23.

Sourirajan, S., and Kennedy, G. C., 1962, The system H_2O-NaCl at elevated temperatures and pressures: American Journal of Science, v. 260, p. 115-141.

Stoeser, D. B., and Camp, V. E., 1985, Pan-African microplate accretion of the Arabian Shield: Geological Society of America Bull., v. 96, no. 7, p. 817-826.

Stuckless, J. S. and Miesch, A. T., 1981, Postorogenic modeling of a potential uranium source rock, Granite Mountains, Wyoming: U.S. Geological Survey Professional Paper 1225, 39 p.

Stuckless, J. S., Vaughn, R. B., VanTrump, G., Jr., 1985, Trace-element contents of postorogenic granites of the eastern Arabian Shield, Kingdom of Saudi Arabia: Saudi Arabian Deputy Ministry for Mineral Resources-Open File Report USGS-OF-06-2, 49 p. Also, 1986, U.S. Geological Survey Open-File Report 86-261.

Thorton, C. P., and Tuttle, O. F., 1960, Chemistry of igneous rocks. I. Differentiation index. American Journal of Science, v. 258, p. 664-684.

Tischendorf, G., 1977, Geochemical and petrographic characteristics of silicic magmatic rocks associated with rare-element mineralization, in Metallization associated with acid magmatism: Czechoslovakia Geological Survey, Prague, v. 2, p. 41-96.

Tuttle, O. F. and Bowen, N. L., 1958, Origin of granite in the light of experimental studies in the system $NaAlSi_3O_8$- $KAlSi_3O_8$-SiO_2-H_2O: Geological Society of America Memoir 74, 153 p.

Wallace, S. R., Muncaster, N. K., Jonson, D. C., MacKenzie, W. B., Bookstrom A. A., and Surface V., 1968, Multiple intrusion and mineralization at Climax, Colorado: in Ridge, J.D., ed., Ore deposits of the United States, 1933-1967 (Graton-Sales Vol.): New York, American Institute of Mining, Metallurgical and Petroleum Engineers, p. 605-640.

White, D. E. and Waring, G. A., 1963, Volcanic emanations; in Data of geochemistry (6^{th} ed.): U.S. Geological Survey Professional Paper 440-K, p. 1-29.

White, W. H., Bookstrom A. A., Kamilli, R. J., Ganster, M. W., Smith, R. P., Ranta, D. E., and Steininger, R. C., 1981, Character and origin of Climax-type molybdenum deposits: Economic Geology 75^{th} Anniversary Volume, p. 270-316.

Winkler, H. G. F., 1967, Petrogenesis of metamorphic rocks: Springer-Verlag New York Inc., 237 p.

APPENDIX

Petrography of analyzed rocks

889494; DDH (diamond drill hole) BAJ-3-100.0

This is the freshest of the four samples analyzed and comes from a dike that cuts the Murdama hornfels near the known eastern limit of the Baid al Jimalah West deposit. The rock is coarsely porphyritic with a hypidiomorphic-granular, seriate groundmass. Perthitic alkali feldspar, quartz, and plagioclase phenocrysts comprise about 15 percent of the rock. The qroundmass is composed of perthitic alkali feldspar (ca. 40 percent), quartz (ca. 33 percent), albite (ca. 20 percent), and biotite (ca. 5 percent). Albite is weakly sericitized and some of the alkali feldspar has been very weakly albitized. The biotite shows various stages of alteration to coarse muscovite and opaque minerals. The white micas of the veins and greisen alteration were not analyzed; most are probably F-rich muscovite due to the low Li-content of the granite. (See table 2.) Cole and others (1981) report that X-ray diffraction studies revealed the presence of a trioctahedral mica (lepidolite?, zinnwaldite?) plus traces of topaz and tourmaline in heavy mineral separates from crushed greisen material. The paucity of fluid inclusions, almost all of which are liquid-rich and contain small (i.e. low temperature) bubbles, is consistent with this rock being only weakly altered.

893039; BAJ-6-47.9 to 48.9

Incipient greisenization, in addition to weak sericitization, is characteristic of this sample, the most altered of the four. Its texture and primary mineralogy are virtually identical with sample no. 889494, but about 50 percent of the albite is replaced by sericite. About 1 percent of the alkali feldspar and all of the biotite has been replaced by coarse muscovite. Traces of pyrite and a carbonate are common. Many more fluid inclusions are apparent than in sample no. 889494. They are liquid-rich, but with large bubbles, indicating that this rock has been appreciably affected by greisenizing fluids (Stages 3 and 4). Rare, 3-phase H_2O-CO_2 fluid inclusions were observed, along with groups of vapor- and liquid-rich, low temperature inclusions.

893159; BAJ-6-166.2 to 166.7

This sample comes from near the top of the main cupola, where there are sharp variations in phenocryst content and groundmass size. It is markedly different in texture from the other samples because it is characterized by an aplitic groundmass. Perthitic alkali feldspar, quartz, and albite phenocrysts comprise about 12 percent of the rock. The quartz phenocrysts show some evidence of resorbtion. The groundmass is composed of quartz (ca. 38 percent), alkali feldspar (ca. 40 percent), and albite (ca. 10 percent). The alkali feldspar is weakly sericitized and the albite is moderately sericitized. Very little biotite remains; most has been altered to muscovite, plus traces of carbonate and opaque minerals. This rock is intermediate in intensity of alteration between the two previously discussed. No evidence of greisenization was observed. Fluid inclusions are mostly low temperature and liquid-rich. Some vapor-rich and 3-phase H_2O-CO_2 fluid inclusions are also present.

893235; BAJ-6-246.2 to 247.2

This sample is the from the bottom of the drill hole in the cupola, about 180 meters below the surface, and represents the deepest penetration of the Baid al Jimalah system. The rock is porphyritic, with about 8 percent total phenocrysts (perthitic alkali feldspar, albite, and quartz). There are two separate groundmasses: one is seriate, hypidiomorphic-granular and is similar to that seen in in samples no. 889494 and 893039; the other, comprising less than ten percent, is aplitic. The type and intensity of alteration is the same as in sample no. 893159.